Remarkable dominance of myctophid otoliths indicates Caribbean coastal upwelling in late Miocene Panama

Chien-Hsiang Lin [Corresp., 1], **Aaron O'Dea** [2, 3]

[1] Biodiversity Research Center, Academia Sinica, Taipei, Taiwan

[2] Smithsonian Tropical Research Institute, Panama City, Panama

[3] Sistema Nacional de Investigación, Panama City, Panama

Corresponding Author: Chien-Hsiang Lin
Email address: chlin.otolith@gmail.com

Marine fossils from the late Miocene Chagres Formation in northern Panama offer critical insights into the paleoenvironmental conditions and ecological responses just prior to the separation of the Atlantic from the Pacific by the formation of the Isthmus of Panama. Here we present a systematic study based on more than 6,200 otoliths collected from a coastal exposure near the town of Piña, Colón. This assemblage is remarkable for the extraordinary dominance of the family Myctophidae, constituting over 96% of specimens. The otolith density in the sediments is the richest known globally. The taxonomic composition is represented by 31 taxa across 12 families, including four newly described species, namely *Chiloconger aflorens* sp. nov., *Dasyscopelus inopinatus* sp. nov., *Hoplostethus boyae* sp. nov., and *Malakichthys schwarzhansi* sp. nov. Taphonomic evidence, combined with abundant predatory marine vertebrate fossils and extensive burrow ichnofossils, indicates a dynamic and highly productive near-shore ecosystem. The dominance of myctophids and multiple lines of evidence support the existence of a late Miocene coastal upwelling system in the region, highlighted by efficient trophic transfer channeled from high primary production to apex predators. These findings provide a nuanced understanding of Neogene marine ecosystems prior to the final emergence of the Isthmus of Panama.

Remarkable dominance of myctophid otoliths indicates Caribbean coastal upwelling in late Miocene Panama

Chien-Hsiang Lin[1], Aaron O'Dea[2,3]

[1] Biodiversity Research Center, Academia Sinica, Taipei 11529, Taiwan
[2] Smithsonian Tropical Research Institute, Balboa, 0843, Republic of Panamá
[3] Sistema Nacional de Investigación (SENACYT), Panamá, Republic of Panamá

Corresponding Author:
Chien-Hsiang Lin[1]
Biodiversity Research Center, Academia Sinica, Taipei 11529, Taiwan
Email address: chlin.otolith@gmail.com

Abstract

Marine fossils from the late Miocene Chagres Formation in northern Panama offer critical insights into the paleoenvironmental conditions and ecological responses just prior to the separation of the Atlantic from the Pacific by the formation of the Isthmus of Panama. Here we present a systematic study based on more than 6,200 otoliths collected from a coastal exposure near the town of Piña, Colón. This assemblage is remarkable for the extraordinary dominance of the family Myctophidae, constituting over 96% of specimens. The otolith density in the sediments is the richest known globally. The taxonomic composition is represented by 31 taxa across 12 families, including four newly described species, namely *Chiloconger aflorens* sp. nov., *Dasyscopelus inopinatus* sp. nov., *Hoplostethus boyae* sp. nov., and *Malakichthys schwarzhansi* sp. nov. Taphonomic evidence, combined with abundant predatory marine vertebrate fossils and extensive burrow ichnofossils, indicates a dynamic and highly productive near-shore ecosystem. The dominance of myctophids and multiple lines of evidence support the existence of a late Miocene coastal upwelling system in the region, highlighted by efficient trophic transfer channeled from high primary production to apex predators. These findings provide a nuanced understanding of Neogene marine ecosystems prior to the final emergence of the Isthmus of Panama.

Introduction

The formation of the Isthmus of Panama is recognized as a critical event that fundamentally shaped modern ocean circulation, biogeographic patterns, and the evolutionary history of both terrestrial and marine organisms (Haug & Tiedemann, 1998; O'Dea et al., 2016; Jackson & O'Dea, 2023; Titus et al., 2024). Localized tectonic fracturing, faulting and extension, as well as subduction-driven uplift during the formation of the isthmus resulted in numerous marine

sedimentary basins to develop, initially as interconnected fore- and back-arc basins along an extended archipelago (Farris et al. 2011). Continued uplift and volcanic "infilling" (Buchs et al. 2019) eventually led to the isthmus forming a complete marine barrier in the late Pliocene around 2.8 Ma (O'Dea et al., 2016). These sedimentary basins are crucial repositories of Neogene fossils, which have been helpful in revealing patterns of change in the diversity, ecology and evolution of marine faunas through a major environmental transition (Jackson & O'Dea, 2023).

Marine sedimentary archives often contain fish otoliths which offer unique insights into the spatiotemporal distribution, community structure, and evolutionary history of fishes (Nolf, 2013). In Tropical America, multiple studies have been conducted on Neogene otolith, including Schubert (1908) and Martin & Dunn (2000) in Panama, Nolf (1976) in Trinidad, Nolf & Stringer (1992) in the Dominican Republic, Nolf & Aguilera (1998) and Aguilera && Rodrigues de Aguilera (2001, 2003) in Venezuela, and Aguilera et al. (2014) in Brazil. Studies by Schwarzhans & Aguilera (2013, 2016, 2024) and Aguilera et al. (2016; 2020) have comprehensively described otoliths of multiple families from tropical America, including material from Panama. Nonetheless, the upper Miocene Chagres Formation, one of the significant fossil-yielding strata associated with the final stages of isthmus formation (Stiles et al., 2022), has not been thoroughly investigated for its otolith assemblage at the community level.

The depositional environment of Chagres Formation was originally interpreted as a deep-water setting with notable Pacific influence (Collins & Coates, 1993; Coates & Obando, 1996), based primarily on the composition of benthic foraminifera (Collins et al., 1996, 1999), elasmobranch teeth (Carrillo-Briceño et al., 2015), and teleost otoliths (Aguilera & Rodrigues de Aguilera, 1999). Conversely, recent studies of ichnofossils and sedimentological data have proposed a relatively shallow-water depositional environment (Stiles et al., 2022).

In this study, we present results from quantitative otolith sampling from the Chagres Formation on the Caribbean coast of Panama. Based on the collection of over 6,200 otoliths, we document the richest fish records from the upper Miocene of the Panama Canal Basin. We provide detailed taxonomic remarks, assess taphonomic conditions, reconstruct paleoenvironmental contexts, and discuss trophic dynamics from a paleoecological perspective.

Geological setting

The Panama Canal Basin is underlain primarily by Cretaceous volcanic and plutonic rocks, which reflects its volcanic arc origins (Coates & Obando, 1996; Coates, 1999). Overlying this basement is a series of Cenozoic sedimentary formations, and the extensive Neogene transisthmian marine sediments were exposed during the construction of the Panama Canal (Woodring, 1957). Sediment deposition within the basin is structurally controlled by the Gatun Fault Zone, which separates the Chorotega Block in western Panama and the Choco Block in the east (Coates & Obando, 1996; Coates, 1999).

On the Caribbean side of Colón Province, Panama, the Neogene deposits are primarily represented by the Gatun Formation and the overlain Chagres Formation (Coates, 1999). The Gatun Formation is of late middle to late Miocene (Hendy, 2013), consists of approximately 500 m of massive, blue-gray, marine fine sandstone to siltstone, notable for its rich and diverse marine fossils, particularly the mollusk fossils (Woodring, 1957; Jackson et al., 1999). Fossil evidence indicates deposition occurred at relatively shallow marine depths, typically less than 40 m (Coates & Obando, 1996; Collins et al., 1999).

The Chagres Formation, deposited between approximately 6.4 and 5.8 Ma (Collins et al., 1996), is predominantly exposed in the northern part of the Panama Canal Zone and extends southwestward along the Caribbean coast (Fig. 1). The formation is about 250 m thick and primarily comprises marine, blue-gray volcaniclastic sandstone derived from volcanic arcs (Collins et al., 1996; Coates, 1999). It is subdivided into three members: the basal Toro Limestone, the intermediate Rio Indio Siltstone, and the upper Chagres Sandstone. The Toro Limestone Member is characterized by calcareous beds rich in coquina composed of echinoid, mollusk, and barnacle fragments (Coates, 1999; Stiles et al., 2022). The Chagres Sandstone Member consists of gray, quartzose, volcanic-derived silty sandstones that exhibit extensive bioturbation, predominantly from arthropod burrows (Collins et al., 1996; Stiles et al., 2022). These sandstones yield abundant marine fossils and are prominently exposed along the Caribbean coast (Aguilera & Rodrigues de Aguilera, 1999; Carrillo-Briceño et al., 2015; Pyenson et al., 2015; Velez-Juarbe et al., 2015; Stiles et al., 2022; Benites-Palomino et al., 2023; Cadena, Gracia & Combita-Romero, 2023), particularly near the town of Piña (see below).

Materials & Methods

Sampling

The fossil site is located about ~500 m northeast of Piña town, Colón, Panama (Fig. 1; 9°17'09.11"N, 80°02'41.28"W). This locality corresponds to the Piña Norte site described by Stiles et al. (2022) and the STRI site 650009 in Pyenson et al. (2015). The Chagres Sandstone Member of the Chagres Formation is exposed along the Caribbean shoreline, especially at low tide (Fig. 2B). Fragments of echinoids, mollusks, and fish otoliths, as well as trace fossils, are easily visible on the surface of the siltstone (Stiles et al., 2022). Surface sediments are yellowish to brownish, contrasting with fresh sediments located several centimeters below the surface, which are darker and have a distinct blue-gray color. We collected thirty-three bulk sediment samples from the fresher, blue-grey material in 2018 and 2024. Samples weighed on average 0.6 kg each (Table S1). An additional larger bulk sample (unweighted) was also collected from this fresh sandstone layer for otolith extraction (Table S1). Permits for collecting and exporting paleontological samples were issued by the Ministerio de Comercio e Industrias (MICI, SE/AO-4-18) in Panamá.

Otolith preparation, imaging, and identification

Bulk sediment samples were disaggregated using freeze-thaw cycles and Glauber's Salt (saturated sodium sulfate solution) methods (Hanna & Church, 1928; Herrig, 1966), then wet-sieved through a 500-μm mesh. After sieving, sediments were dried overnight in an oven at 40°C. Otoliths larger than this 500-μm mesh were carefully hand-picked under a stereomicroscope. In this study, the term "otolith" refers to the saccular otolith (sagitta). Representative otoliths were photographed using a digital camera adapted to a Nikon SMZ1270 stereomicroscope, and image stacking was performed using Helicon Focus software. Final figures were prepared using Adobe Photoshop.

For otolith identification and terminology, we followed key references, including Rivaton & Bourret (1999), Lin & Chang (2012), Schwarzhans (2013), Schwarzhans & Aguilera (2013, 2016), Nolf (2013), and Haimovici et al. (2024). In addition, direct comparisons were made with a reference collection of extant otoliths housed at the Biodiversity Research Museum, Academia Sinica, Taiwan (BRCAS) under the code CHLOL. Whenever possible, otoliths were identified to the species level. All collected specimens are stored at BRCAS, and figured specimens are archived under the registration code ASIZF.

Biodiversity analysis

Due to the overwhelming number of otoliths in each sample, we conducted biodiversity analysis to assess sampling completeness and diversity. Otolith abundance was quantified by dividing otolith counts by the corresponding dry sediment weight (kg) for each sample. Diversity was measured using Hill numbers (Hill, 1973) calculated at three different orders: $q = 0$ (${}^0D$, species richness), $q = 1$ (${}^1D$, Shannon diversity), and $q = 2$ (${}^2D$, Simpson diversity), representing total (alpha) species richness, abundant species diversity, and dominant species diversity, respectively (Chao, Chiu & Jost, 2014; Chao et al., 2020; Lin et al., 2023a). Rarefaction and extrapolation methods were applied to create species accumulation curves, with 1,000 bootstrap resampling iterations used to estimate 95% confidence intervals. Specimen-based abundance data was analyzed to evaluate sample coverage comprehensively. All analyses were conducted using the R package iNEXT (Chao, Chiu & Jost, 2014; Hsieh, Ma & Chao, 2016).

Nomenclatural acts for new species

The electronic version of this article in Portable Document Format (PDF) will represent a published work according to the International Commission on Zoological Nomenclature (ICZN), and hence the new names contained in the electronic version are effectively published under that Code from the electronic edition alone. This published work and the nomenclatural acts it contains have been registered in ZooBank, the online registration system for the ICZN. The ZooBank LSIDs (Life Science Identifiers) can be resolved and the associated information viewed through any standard web browser by appending the LSID to the prefix http://zoobank.org/. The LSID for this publication is: urn:lsid:zoobank.org:pub:996A25D1-9CB7-4AAD-9041-0ABCF49710C5. The online version of this work is archived and available from the following digital repositories: PeerJ, PubMed Central and CLOCKSS.

Results

Systematic Paleontology

A list of identified taxa and their abundances is presented in Table 1. Classification scheme follows Nelson et al. (2016). Morphometrics and measurements include otolith length (OL), otolith height (OH), sulcus length (SuL), ostium length (OsL), and cauda length (CaL). Descriptions and discussions for common or previously described taxa are provided briefly under remarks, while new species include detailed descriptions and diagnostics.

Order Anguilliformes
Family Congridae
Genus *Chiloconger* Myers & Wade, 1941
Chiloconger aflorens sp. nov.
(Figs. 3A–3B)

Holotype: ASIZF 0100943 (Fig. 3A), Piña Norte, Panama. Late Miocene, Chagres Formation.
Paratypes: One specimen: ASIZF 0100944 (Fig. 3B), same data as holotype.
Etymology: The species name *aflorens* is derived from the Spanish word “afloramiento”, meaning "upwelling." It refers to the flourishing productivity and dynamic marine conditions of the coastal upwelling system in which this species lived. It also symbolically reflects the scientific blossoming of paleontological research in Panama.
Diagnosis: OL/OH = 1.25–1.33, OL/SuL = 1.54–1.82. Otoliths oval with thick profile. Dorsal rim dome-shaped, evidently elevated anterior to midline; ventral rim smoothly curved. Sulcus moderately wide, poorly differentiated into ostium and cauda. Cauda short with an obtuse posterior tip.
Description: Otoliths oval to elliptic, thick; inner and outer faces highly convex. Anterior and posterior rims pointed in holotype, blunt to nearly vertical in juvenile paratype. Dorsal rim dome-shaped, elevation just anterior to midline. Ventral rim smoothly curved. Sulcus median, very slightly inclined, poorly divided into ostium and cauda. Ostial channel nearly indiscernible in holotype, but narrow, vertical, and ending just before dorsal elevation in paratype. Cauda short, extending slightly posterior to dorsal elevation; bears obtuse, truncated posterior end.
Remarks: *Chiloconger* is distinguished from other congrids by the notably short cauda, a character state considered plesiomorphic (Schwarzhans 2019; Schwarzhans & Nielsen, 2021). Although based on a subadult specimen, the new species differs from the two extant species, *C. dentatus* (Garman, 1899) and *C. philippinensis* Smith & Karmovskaya, 2003, by having a less pronounced, more anteriorly positioned dorsal elevation (Schwarzhans, 2019). Additionally, compared to the Early Miocene *Chiloconger chilensis* Schwarzhans & Nielsen, 2021 from Chile (Schwarzhans & Nielsen, 2021), *C. aflorens* exhibits a more compact and rounded shape with a less elongated form.
Occurrence: Currently known only from the type locality.

Genus *Rhynchoconger* Jordan & Hubbs, 1925
Rhynchoconger sp.
(Fig. 3C)

Remarks: A single, fragmentary otolith exhibiting key *Rhynchoconger* characteristics is identified to the genus level. The preserved portion shows a discernible ostial channel and anterior ostium outline, both diagnostic for *Rhynchoconger* (Schwarzhans, 2019). Due to the incomplete preservation, further species-level identification is not possible.

Order Argentiniformes
Family Argentinidae
Genus *Argentina* Linnaeus, 1758
Argentina sp.
(Fig. 3D)

Remarks: A single thin otolith is assigned to the genus Argentina based on a strong, nearly right-angled posterodorsal angle, a straight posterior rim, a curved ventral rim, and a median, horizontally oriented sulcus. The anterior portion of the specimen is missing, preventing confident assignment to species level.

Order Stomiiformes
Family Sternoptychidae
Genus *Polyipnus* Günther, 1887
Polyipnus sp.
(Figs. 4A–4B)

Remarks: *Polyipnus* otoliths are distinctive by their tall, compressed shape, indistinctive sulcus outline, elevated colliculum crest along the crista inferior, and a considerable thickness in the posterior rim. However, species-level identification is challenging due to extensive interspecific overlap and the limited availability of modern otolith reference material from the region. Additionally, most specimens from the Chagres Formation are poorly preserved, with only the thick posterior rims preserved. The better-preserved specimens are depicted here.

Order Myctophiformes
Family Myctophidae

Remarks: The abundance of myctophid otoliths in the Chagres Panama is extraordinary. Most identifications are based on large subadult to adult individuals; tentative assignments for juvenile or poorly preserved specimens were conservative, resulting in a significant number of otoliths

classified as Myctophidae indet. Consequently, the true myctophid diversity is likely underestimated in this collection. Significant advances in myctophid otolith taxonomy, sourced by the development of comprehensive global reference collections (Rivaton & Bourret, 1999; Schwarzhans, 2013), have greatly improved identification in fossil assemblages (Schwarzhans et al., 2022; Lin et al., 2023b). We primarily follow Schwarzhans & Aguilera (2013) for taxonomic treatment and species-level identification of the myctophid otoliths in this study.

Genus *Benthosema* Goode & Bean, 1896

Benthosema pluridens Schwarzhans & Aguilera, 2013

(Fig. 4C)

2013 *Benthosema pluridens*; Schwarzhans & Aguilera: pl. 1, figs. 8–12.

Remarks: Otoliths of *B. pluridens* are relatively common in the collection. They are characterized by a sub-rectangular outline, a relatively flat dorsal rim, and multiple ventral denticles. However, juvenile myctophid otoliths often display intermediate outlines between rounded and sub-rectangular forms. To ensure accuracy, only specimens closely matching those illustrated by Schwarzhans & Aguilera (2013: pl. 1, figs. 8–12) were assigned to *B. pluridens*; other, less definitive specimens were conservatively classified under Myctophidae indet. Therefore, the true abundance of *B. pluridens* may be underestimated.

Genus *Bolinichthys* Paxton, 1972

Bolinichthys sp.

(Fig. 4D)

Remarks: A single, juvenile otolith is assigned to *Bolinichthys* based on its prominent rostrum and gently curved, oblique posterior rim, consistent with diagnostic features of the genus (Rivaton & Bourret, 1999). Notably, *Bolinichthys* otoliths have not been previously reported from the Neogene of tropical America (Schwarzhans & Aguilera, 2013).

Genus *Dasyscopelus* Günther, 1864

Remarks: Following the molecular phylogenetic revision by Martin et al. (2018), seven species previously assigned to *Myctophum* (*M. asperum*, *M. brachygnathos*, *M. lychnobium*, *M. obtusirostre*, *M. orientale*, *M. selenops*, and *M. spinosum*) were reallocated to *Dasyscopelus*. We adopt this updated classification herein, although we note that, in our view, otolith morphology among these species does not consistently show clear differentiation from other *Myctophum* species or internally within *Dasyscopelus* itself (see Schwarzhans & Aguilera, 2013: pl. 3). Otoliths attributed to *Dasyscopelus* are typically characterized by a pronounced posterior extension and a pointed ventral rim, giving them a more angular appearance compared to the generally rounded and often deeper-bodied otoliths of *Myctophum*. Exceptions include *D.*

brachygnathos and *D. selenops*, which possess a much shorter posterior rim and a taller overall shape (Schwarzhans & Aguilera, 2013; Ng et al., 2024a).

Three closely related species—*Dasyscopelus degraciai* (Schwarzhans & Aguilera, 2013), *Dasyscopelus jacksoni* (Aguilera & Rodrigues de Aguilera, 2001), and the newly described *Dasyscopelus inopinatus* sp. nov. (see below)—are here allocated to the genus *Dasyscopelus* due to their otoliths having a protruding posterior part, a relatively flat dorsal rim, and general similarity to extant *Dasyscopelus* species, such as *D. asper* and *D. lychnobius*.

Dasyscopelus degraciai (Schwarzhans & Aguilera, 2013)
(Figs. 5A–5F)
2013 *Myctophum degraciai*; Schwarzhans & Aguilera: pl. 5, figs. 1–5.

Remarks: The otoliths of *D. degraciai* are distinguished by their compact outline, less pronounced posterior extension, gently curved dorsal rim, and narrower sulcus. They differ from the co-occurring *D. inopinatus* sp. nov. and the Pliocene *D. jacksoni* by their shorter posterior rim and more compact, less angular shape.

Dasyscopelus inopinatus sp. nov.
(Figs. 5G–5L)

Holotype: ASIZF 0100962 (Fig. 5I), Piña Norte, Panama. Late Miocene, Chagres Formation.
Paratypes: Five specimens: ASIZF 0100957–0961 (Figs. 5G–5H, 5J–5L), same data as holotype.
Additional material: 57 specimens, unfigured, same data as holotype.
Etymology: From Latin *inopinatus* (feminine *inopinata*) = unexpected, alludes to the surprising and remarkable discovery of this new species, which exhibits a mosaic of morphological features shared with closely related congeners.
Diagnosis: OL/OH = 1.39–1.64, OL/SuL = 1.17–1.26, OsL/CaL = 1.45–2.09. Elongate otoliths with thin profile. Dorsal rim flat, nearly horizontal, with slight or no posterior elevation and a postero-dorsal angle. Ventral rim curved, bearing around eight lobes or denticles. Posterior rim short, nearly vertically straight. Sulcus very wide, with large, rectangular ostium and squarish cauda.
Description: Otoliths elongate, thin; both inner and outer faces are relatively flat. Anterior rim bearing large, protruding rostrum and shorter but conspicuous antirostrum, separated by clearly defined notch, varies from shallow to deep. Dorsal rim nearly horizontally flat, occasionally slightly elevated posteriorly, forming postero-dorsal angle just anterior to marked postero-dorsal concavity. Posterior rim short and nearly vertically straight. Ventral rim broadly curved, bearing ~8 lobes or denticles. Sulcus wide, median-positioned. Ostium large, deep, rectangular; cauda short, squarish.

Remarks: The otoliths of the new species exhibit an intermediate morphology between *D. degraciai* and *D. jacksoni*. They share with *D. degraciai* a compact, deep-bodied outline and a less elongate posterior part, but resemble *D. jacksoni* in having a horizontal dorsasl rim, wide sulcus, and a postero-dorsal concavity. Notably, the original illustrations of *D. jacksoni* (as *Lampadena jacksoni* in Aguilera & Rodrigues de Aguilera, 2001: figs. 7.15–7.22) suggest a more elongated and posteriorly extended shape compared to the ones documented in Schwarzhans & Aguilera (2013: pl. 5, figs. 6–10), as also indicated by differences in OL/OH ratios (1.60–1.86 vs. 1.50–1.65), although this may reflect ontogenetic variation.

Schwarzhans & Aguilera (2013) proposed a species turnover from the late Miocene *D. degraciai* to the Pliocene *D. jacksoni* at the boundary between Messinian and Zanclean and further suggested a linear relationship between the two species. However, the finding of *D. inopinatus* suggests a more complex evolutionary history, with this new species likely representing a transitional or closely related lineage to *D. jacksoni*.

Occurrence: Currently known only from the type locality.

Genus *Diaphus* Eigenmann & Eigenmann, 1890

Remarks: *Diaphus* represents the most abundant and diverse taxon in our collection. A total of seven species, *D. aequalis*, *D. apalus*, *D. barrigonensis*, *D. dumerilii*, *D. multiserratus*, *D. pedemontanus*, and *D. rodriguezi*, are recorded. Our identifications are primarily based on larger, more mature specimens, which exhibit sufficient diagnostic characters to allow confident assignment (see remarks under the family). The otolith taxonomy of *Diaphus* has been extensively revised by Schwarzhans & Aguilera (2013), whose detailed descriptions and high-quality images serve as the primary references for this study. Therefore, only brief remarks distinguishing among similar co-occurring species are presented here.

Diaphus aequalis Schwarzhans & Aguliera, 2013

(Figs. 6A–6C)

1992 *Diaphus* aff. *D. brachycephalus* Tåning, 1928; Nolf & Stringer: pl. 10, figs. 11–13.

?1992 *Diaphus* sp. 1; Nolf & Stringer: pl. 10, fig. 19.

1998 *Diaphus brachycephalus* Tåning, 1928; Stringer: pl. 2, fig. 2.

2013 *Diaphus aequalis*; Schwarzhans & Aguilera: pl. 13, figs. 13–25.

Remarks: The species is common but never abundant within the Piña assemblage. Its otoliths are morphologically most similar to smaller individuals of the co-occurring *D. apalus* and, to a lesser extent, *D. barrigonensis* (see below). It differs from *D. apalus* by its very rounded and compact outline, and by possessing only a subtle postero-dorsal concavity (vs. a pronounced, deeply indented concavity). Compared to *D. barrigonensis*, *D. aequalis* is distinguished by its shorter rostrum and gently curved dorsal and posterior rims (vs. steeply inclined dorsal rim and sharp posterior rim).

Diaphus apalus Schwarzhans & Aguliera, 2013
(Figs. 6D–6F)
2013 *Diaphus apalus*; Schwarzhans & Aguilera: pl. 13, figs. 1–10.

Remarks: See remarks under *D. aequalis*.

Diaphus barrigonensis Schwarzhans & Aguliera, 2013
(Figs. 6G–6K)
2001 *Diaphus* sp. 2; Aguilera & Rodrigues de Aguilera: fig. 7.7–7.8.
2013 *Diaphus barrigonensis*; Schwarzhans & Aguilera: pl. 7, figs. 1–9.

Remarks: See remarks under *D. aequalis*.

Diaphus dumerilii (Bleeker, 1856)
(Figs. 6L–6O)
?1976 *Diaphus dumerilii* (Bleeker, 1856); Nolf: pl. 3, figs. 8–14.
1992 *Diaphus* sp. 1; Nolf & Stringer: pl. 10, figs. 18, 20–21, 23 (non figs. 19, 22).
1998 *Diaphus* sp. 1; Stringer: pl. 2, fig. 3.
2001 *Diaphus dumerilii* (Bleeker, 1856); Aguilera & Rodrigues de Aguilera: figs. 7.1–7.2.
2013 *Diaphus dumerilii* (Bleeker, 1856); Schwarzhans & Aguilera: pl. 10, figs. 18–23.

Remarks: The otoliths of *D. dumerilii* are most recognizable by their slightly elevated antero-dorsal rim and the narrow antero-ventral part of the rostrum. However, as noted by Schwarzhans & Aguilera (2013), these otoliths are morphologically inconspicuous and, in our view, confident identification is generally limited to larger, well-preserved specimens. Some otoliths assigned to *D. dumerilii* by Nolf (1976) from Neogene deposits in Trinidad display a more compact outline (e.g., pl. 3, figs. 8, 11–12), suggesting they may actually belong to different species. Nevertheless, distinguishing such variations based solely on the available figures remains difficult.

Diaphus multiserratus Schwarzhans & Aguliera, 2013
(Figs. 7A–7B)

2013 *Diaphus multiserratus*; Schwarzhans & Aguilera: pl. 12, figs. 4–11.

Remarks Otoliths of *D. multiserratus* are readily distinguished by their elongate outline, wide sulcus, and, most conspicuously, the presence of numerous minute denticles along the ventral rim. Although not a frequent species in the collection, it is typically represented by larger, well-preserved specimens.

Diaphus pedemontanus (Robba, 1970)
Fig. 7C–F

1970 *Porichthys pedemontanus*; Robba: pl. 16, fig. 8.
2013 *Diaphus pedemontanus* (Robba, 1970); Schwarzhans & Aguilera: pl. 9, figs. 1–4.

Remarks: *Diaphus pedemontanus* closely resembles the co-occurring and most abundant species *D. rodriguezi*, but can be distinguished by a high, more undulating dorsal rim and a short, nearly vertically straight posterior rim, whereas *D. rodriguezi* has a gently curved dorsal rim, a deeper and wider excisura, and a larger rostrum (see below). Otoliths of *D. pedemontanus* are widely recorded from the Miocene and Pliocene of the Mediterranean (Girone, Nolf & Cavallo, 2010; Lin, Girone & Nolf, 2015; Lin et al., 2017) and have also been documented in the coeval Caribbean assemblages (Schwarzhans & Aguilera, 2013). Ontogenetic variation in *D. pedemontanus* is considerable (Brzobohatý & Nolf, 2000), although we note that Caribbean specimens tend to be smaller than their European counterparts.

Diaphus rodriguezi Schwarzhans & Aguliera, 2013
(Figs. 7G–7J)

2013 *Diaphus rodriguezi*; Schwarzhans & Aguilera: pl. 9, figs. 5–12.

Remarks: See remarks under *D. pedemontanus*.

Genus *Diogenichthys* Bolin, 1939
Diogenichthys sp.
(Fig. 7K)

Remarks: A single otolith, characterized by a rounded outline (OL/OH = 1.04) and a thick profile, is assigned to the genus *Diogenichthys* (see Schwarzhans & Aguilera, 2013). However, due to partial damage along the anterior rim and the absence of additional material for comparison, species-level identification was not attempted.

Genus *Lepidophanes* Fraser-Brunner, 1949
Lepidophanes inflectus Schwarzhans & Aguliera, 2013
(Fig. 8I)

2001 *Lampanyctus* aff. *latesulcatus* Nolf & Stringer, 1992; Aguilera & Rodrigues de Aguilera: figs. 7.13–7.14. (note: the authorship of *L. latesulcatus* should be Nolf & Steurbaut, 1983).
2013 *Lepidophanes inflectus*; Schwarzhans & Aguilera: pl. 6, figs. 16–19.

Remarks: Otoliths of this species are very small, but highly diagnostic within the assemblage. They are particularly recognized by a subtle ventral inflection along the ostial crista inferior, although this feature is variably preserved among specimens. These otoliths also resemble much to those of *Lampanyctus latesulcatus* from the Tortonian Mediterranean; however, *L. latesulcatus* displays a more compact outline and lacks the ventral inflection characteristic of *L. inflectus* (Nolf & Steurbaut, 1983).

Genus *Lobianchia* Gatti, 1904
Lobianchia johnfitchi Schwarzhans & Aguliera, 2013
(Figs. 8A–8C)

2013 *Lobianchia johnfitchi*; Schwarzhans & Aguilera: pl. 14, figs. 10–15.

Remarks: *Lobianchia johnfitchi* is readily distinguished from other myctophid otoliths by its wide sulcus, prominently elevated antero-dorsal rim, and strongly depressed postero-dorsal rim. A closely related extant congener, *L. dofleini* (Zugmayer, 1911), exists during the Miocene–Pliocene in the NE Atlantic and Mediterranean (Lin et al., 2017). We follow Schwarzhans & Aguilera's (2013) interpretation that *L. johnfitchi* persisted in the Caribbean until the middle Pliocene, whereas *L. dofleini* continued its presence into the modern Atlantic and Mediterranean.

Genus *Myctophum* Rafinesque, 1810
Myctophum affine (Lütken, 1892)
(Figs. 8G–8H)

1992 *Myctophum* sp.; Nolf & Stringer: pl. 10, figs. 14–15.
2013 *Myctophum affine* (Lütken, 1892); Schwarzhans & Aguilera: pl. 4, figs. 9–12.

Remarks: *Myctophum affine* is recognized by its very rounded and relatively flat otolith outline. The specimens from the Piña assemblage agree well with extant *M. affine* otoliths (Nolf & Stringer: pl. 10, figs. 16–17; Schwarzhans & Aguilera: pl. 3, figs. 17–18). It differs from the closely related fossil species *Myctophum arcanum* Schwarzhans & Aguliera, 2013 by having a shorter posterior extension and a slightly curved dorsal rim (see below).

Myctophum arcanum Schwarzhans & Aguliera, 2013
(Figs. 8D–8F)

2013 *Myctophum arcanum*; Schwarzhans & Aguilera: pl. 4, figs. 13–17.

Remarks: See remarks under *M. affine*.

Order Gadiformes
Family Macrouridae
Genus *Coelorinchus* Giorna, 1809
Coelorinchus sp.
(Figs. 9A–9B)

Remarks: Two incomplete otoliths are assigned to *Coelorinchus* based on the presence of the characteristic pince-nez-shaped sulcus and the presence of a collicular crest at the collum. However, due to the fragmentary preservation, further identification beyond the genus level is not possible.

Family Bregmacerotidae
Genus *Bregmaceros* Tompson, 1840
Bregmaceros sp.
(Figs. 9C–9E)

Remarks: *Bregmaceros* otoliths are the third most common family in the Piña assemblage, although nearly all specimens are poorly preserved. They typically show a heavily abraded inner surface, such that the ostial and caudal depressions are not preserved (Figs. 9C–9D), while the general outline remains intact, complicating detailed taxonomic assignment. The only and best-preserved specimen is illustrated in Fig. 9E. Due to their preservation state, the specimens are conservatively identified only to the genus level.

Order Trachichthyiformes
Family Trachichthyidae
Genus *Hoplostethus* Cuvier, 1829
Hoplostethus boyae sp. nov.
(Figs. 10A–10D)

Holotype: ASIZF 0101006 (Fig. 10A), Piña Norte, Panama. Late Miocene, Chagres Formation.
Paratypes: Three specimens: ASIZF 0101007–1009 (Figs. 10B–10D), same data as holotype.
Etymology: Named in honor of Brígida De Gracia (Boya in Ngäbere, the language of the Ngäbe-Buglé people) for her outstanding contributions to scientific research, public communication, and outreach activities in Panamá.
Diagnosis: OL/OH = 0.99–1.17, OL/SuL = 1.14–1.24, OsL/CaL = 0.72–0.88. Tall, sole-shaped otoliths with thick profile. Dorsal rim dome-shaped, evidently elevated posterior to midline; ventral rim either horizontally straight or smoothly curved, occasionally with large undulations.

Sulcus very broad, shallow, median, well-differentiated into ostium and cauda. Ostium subtriangular, opening widely antero-dorsally. Cauda broad, rectangular.

Description: Otoliths tall, sole-shaped, thick; outer face strongly convex, inner face nearly flat. Dorsal rim curved, markedly elevated posterior to midline. Anterior rim with obtuse, upward-directed rostrum. Posterior rim straight, strongly inclined between postero-dorsal and postero-ventral angles, especially pronounced in larger specimens. Ventral rim horizontally straight to smoothly curved, occasionally with large undulations. Sulcus shallow, very broad, median; ostium subtriangular, opening widely antero-dorsally with shallow colliculum; cauda rectangular, broad, shallow. Dorsal depression fan-shaped, moderately deep.

Remarks: Among the six extant *Hoplostethus* species inhabiting the pan-Caribbean and East Pacific (*H. atlanticus*, *H. fragilis*, *H. mediterraneus*, *H. mento*, *H. occidentalis*, and *H. pacificus*), *H. boyae* most closely resembles juvenile otoliths of *H. occidentalis* (Haimovici et al., 2024: p. 139; but see (Conversani et al., 2017): pl. 8). Other extant species typically exhibit a more variable dorsal rim, including flattened or undulating forms, often with digitiform projections, which may be a reflection of ontogenetic variation (Kotlyar, 1996). The new species differs by its consistently gently curved, dome-shaped dorsal rim, observed across both juvenile and adult stages. Compared to fossil congeners, such as the European Miocene species *Hoplostethus praemediterraneus* Schubert, 1905, and the Pliocene *Hoplostethus pisanus* Koken, 1891, *H. boyae* exhibits a more elevated dorsal profile and a shorter posterior rim, making the overall outline more compact and erect.

Occurrence: Currently known only from the type locality.

Order Ophidiiformes

Family Carapidae

Genus *Carapus* Rafinesque, 1810

Carapus sp.

(Figs. 10E–10F)

Remarks: All *Carapus* otoliths in the Piña assemblage are small and represented by juvenile specimens. They closely resemble an undescribed fossil *Carapus* otolith illustrated by Schwarzhans & Aguilera (2016: fig. 12), although preservation quality in our material is poorer. Given the incomplete preservation and small size, the specimens are conservatively assigned to the genus level. Schwarzhans & Aguilera (2016) further referred to a larger specimen from the Pliocene of Jamaica, depicted by Stringer (1998), but in our view, confirming such a connection requires additional material.

Family Ophidiidae

Genus *Lepophidium* Gill, 1895

Lepophidium limulum Schwarzhans & Aguliera, 2016

(Fig. 10G)

Remarks: A comprehensive review on the otolith taxonomy of fossil Ophidiidae from the region, and particularly the genus *Lepophidium*, has been provided by Schwarzhans & Aguilera (2016). The juvenile otoliths assigned to *Lepophidium limulum* closely match the type material illustrated by Schwarzhans & Aguilera (2016: fig. 56). The species is characterized by a gently declining dorsal rim, a moderately proportioned sulcus with a slight ventral notch at the posterior of cauda.

Order Gobiiformes
Family Opistognathidae
Genus *Opistognathus* Cuvier, 1816
Opistognathus sp.
(Fig. 11A)

Remarks: A peculiar, thickset otolith is assigned to *Opistognathus* based on its distinctive sulcus morphology. The ostium curves sharply upward anteriorly, while the cauda initially bends slightly upward before flexing ventrally in its posterior portion. This sulcus configuration matches the pattern seen in extant *Opistognathus* otoliths (see Nolf & Stringer, 1992: pl. 15, fig. 10). Due to limited material, identification is restricted to the genus level.

Order Carangiformes
Family Carangidae
Carangidae indet.
Fig. 11B)

Remarks: Two thin otoliths are assigned to the family Carangidae based on their pronounced concavity of the outer face and the presence of a typical percomorph-type sulcus. However, due to incomplete preservation, particularly of the anterior regions, further identification to genus or species level was not attempted.

Order Acropomatiformes
Family Malakichthyidae
Genus *Malakichthys* Döderlein, 1883
Malakichthys schwarzhansi sp. nov.
(Figs. 12A–12F)

?1999 *Epigonus denticulatus* Dieuzeide, 1950; (Aguilera & Rodrigues de Aguilera, 1999): pl. 1.

Holotype: ASIZF 0101015 (Fig. 12A), Piña Norte, Panama. Late Miocene, Chagres Formation.
Paratypes: Five specimens: ASIZF 0101016–1020 (Figs. 12B–12F), same data as holotype.

Additional material: Nine specimens, unfigured, same data as holotype.
Etymology: Named in honor of Dr. Werner Schwarzhans (Natural History Museum of Denmark) for his outstanding contributions to the study of fossil and extant fish otoliths, particularly in tropical America.
Diagnosis: OL/OH = 1.12–1.29, OL/SuL = 1.05–1.15, OsL/CaL = 0.59–0.90. Pentagonal otoliths with thick profile. Dorsal rim gently angled, highest anterior to midline; ventral rim gently angled or curved, deepest slightly anterior to midline; posterior rim nearly vertically straight. Sulcus broad, median, shallow, clearly divided into ostium and cauda. Ostium oblong, filled with colliculum, opening widely antero-dorsally. Cauda horizontally straight, narrow, slightly flexed at tip, nearly reaching posterior rim.
Description: Otoliths pentagonal, thick; thickness mostly from convex outer face umbo, inner face slightly convex. Dorsal rim gently angled, highest point anterior to midline, ending in postero-dorsal angle (most manifest in larger specimens). Ventral rim curved or subtly angled, deepest point slightly anterior to midline. Posterior rim nearly vertically straight. Sulcus broad, median, bounded by well-developed cristae. Ostium oblong, filled with colliculum, opening widely antero-dorsally; ostial crista superior markedly bent antero-dorsally, crista inferior gently curving upward. Cauda horizontally straight, narrow, nearly reaching posterior rim, slightly flexed at tip. Dorsal depression shallow, wide.
Remarks: The pentagonal outline of *M. schwarzhansi* is superficially similar to otoliths of several other families, such as Lactariidae and Epigonidae. However, none of these possess the markedly upward-directed ostium and sharply bent ostial crista superior observed in *Malakichthys* (Lin et al., 2023b; Ng et al., 2024b) (Fig. 13). Small specimens of *M. schwarzhansi* also resemble otoliths of *Ambassis* (Ambassidae), but *Ambassis* otoliths differ by having a more pointed posterior rim and a slightly widened caudal tip, features not observed in *Malakichthys* (see Fig. 14).

A large otolith previously illustrated by Aguilera & Rodrigues de Aguilera (1999: pl. 1) may belong to this species, although it shows a more strongly elevated dorsal area, possibly reflecting ontogenetic variation. Additional specimens are needed to confirm this assignment.

The genus *Malakichthys* comprises eight extant species distributed in the Indo-Pacific (Yamanoue & Matsuura, 2004; Ng, Liu & Joung, 2023). Other members of the order Acropomatiformes, such as *Parascombrops*, display much wider geographic and stratigraphic distributions (Schwarzhans & Prokofiev, 2017). The occurrence of *M. schwarzhansi* in the late Miocene of Panama suggests that the genus had a broader Neogene distribution than it does today.
Occurrence: Panama: Upper Miocene, Chagres Formation in Piña Norte, Colon. ?Venezuela: Lower Pliocene, Cubagua Formation, northwestern Venezuela.

Otolith density, sample coverage, and diversity indices

A total of 6,211 otoliths were collected from 34 bulk sediment samples, yielding an average otolith density of 278.80 ± 135.59 otoliths/kg (Table S1). Our otolith collection represented 31

taxa belonging to 12 families, plus nine additional specimens remaining indeterminate (Table 1; Fig. 15). Sample coverage, based on specimen counts, reached 99.87%, indicating a high level of sampling completeness. Rarefaction curves based on species richness (${}^0D$) suggested that the estimated diversity could increase to approximately 35 taxa with additional sampling effort (Fig. 16). However, rarefaction curves for Shannon (${}^1D$) and Simpson (${}^2D$) diversity indices approached asymptotes, indicating that the most abundant and dominant taxa were successfully captured (Fig. 16). This pattern suggests that any additional taxa would likely be rare and ~~low-abundance~~.

Discussion

Taphonomy and preservation

Otoliths are exceptionally abundant at the Piña site and are readily visible on the surface of the exposed sediments. Closer examination reveals that the otoliths are not randomly or evenly distributed but instead exhibit distinct clustering patterns within the sediment layers (Figs. 2C–2D). This clustered distribution suggests that otolith burial was not continuous, but occurred episodically, likely linked to biological processes.

Piscivorous predation, digestion, and subsequent excretion are important processes in the formation of otolith assemblages in marine sediments (Nolf, 1985; Lin et al., 2019; Agiadi et al., 2022). Predator feeding events can result in the accumulation of thousands of otoliths, especially by large predators such as dolphins or tunas (Fitch & Brownell, 1968; Lin et al., 2020). At Piña, fossils of marine predatory mammals (dolphins and predatory whales) as well as piscivorous billfishes are common (Fierstine, 1978; Vigil and Laurito, 2014; Pyenson et al., 2015; De Gracia et al., 2022), supporting a predation-mediated accumulation model. Therefore, the clustered distribution of otoliths in the sediments is consistent with deposition from predator excretions rather than from background mortality or mass mortality events.

Moreover, otoliths appear closely associated with ichnofossils attributed to *Ophiomorpha* (Stiles et al., 2022; Figs. 2C–2D). This suggests that burrowing organisms likely have contributed to otolith concentrations, either by feeding on fish or fecal material and subsequently incorporating otoliths into their burrows, as reported in other fossil contexts (Schwarzhans & Carnevale, 2021).

Surface-exposed otoliths are, on the whole, heavily weathered, often cleaving in half and exposing their whitish internal structure. Better-preserved otoliths were obtained from excavated blue-grey sediments found around 1–10 cm deep into the exposed sediments, depending on the distance from the weathered surface. In cases where lower taxonomic assignment was not possible, this was usually due to specimens being juveniles rather than from poor preservation. Nonetheless, a substantial proportion of specimens are moderately eroded, resulting in loss of outline details and resulted in taphonomic scores of 2 or 3 following Agiadi et al. (2022). This, combined with the prevalence of juvenile specimens, contributed to a relatively high number of otoliths being assigned only to the family level.

Paleoenvironmental and paleoecological implications

The otolith assemblage at Piña is extraordinary in both abundance and composition, providing compelling evidence for a unique paleoenvironmental setting. Otolith densities in the Chagres Sandstone at Piña are exceptionally high, with individual sediment samples frequently exceeding 300 otoliths/kg, and one sample exceeding 775 otoliths/kg (Table S1). To our knowledge, these represent the highest otolith densities ever recorded from fossil assemblages for which sediment weight was systematically measured (c.f. Leonhard & Agiadi, 2023).

This unprecedented abundance coincides with a unique taxonomic dominance, where mesopelagic lanternfishes (Myctophidae) constitute over 96% of otoliths and represent more than 50% of the taxa (18 out of 31). Other mesopelagic fishes, such as hatchetfishes (*Polyipnus*) and codlets (*Bregmaceros*), were also present, albeit at much lower frequencies (each approximately 1.5% of the total otolith counts). Nevertheless, these three mesopelagic families (Myctophidae, Sternoptychidae, and Bregmacerotidae) were the top three most abundant families (Fig. 15) at the site, demonstrating the importance of mesopelagic fauna in what we now understand to be relatively shallow-water deposits.

Indeed, sedimentological evidence and the pervasive presence of ichnofossils at Piña strongly favour a more shallow-water paleoenvironmental interpretation (Stiles et al., 2022) than had previously been assigned based on the presence of mesopelagic fishes. These trace fossils and sedimentary structures point to a dynamic, high-energy setting around 50 m depth (Stiles et al., 2022). We account for this apparent discrepancy by accounting for the presence of strong tropical upwelling which has been documented in contemporaneous formations to west in Bocas del Toro and to the east in the Darien using the $d^{18}O$ variation in fossil shells alongside intracolony variation in cupuladriid bryozoans (O'Dea et al., 2007; Grossman et al., 2019; Jackson & O'Dea, 2023). A contemporaneous upwelling system whose fossil otolith assemblages have been identified from near-shore deposits in northern Venezuela (Aguilera & Rodrigues de Aguilera, 2001) share many taxa with the Piña assemblages, further supporting this interpretation.

The ecological pattern observed at Piña differs substantially from modern temperate upwelling systems like the colder Humboldt and California Currents, where anchovies, sardines, and other small epipelagic fishes typically dominate (Chavez et al., 2003)—taxa almost entirely missing from the Piña assemblages. Instead, we argue that the Piña ecosystem was shaped by three key factors: warm tropical temperatures, high productivity from upwelling, and intense predation pressure. High tropical temperatures would have increased metabolic rates, which when combined with elevated primary productivity from upwelling, would have created conditions where predation rates can be extremely high (c.f. Kordas et al., 2022). This would in turn favour the selective survival of predator-avoiding planktivorous fishes like myctophids, whose diel vertical migrations (feeding at the surface at night and retreating to deeper waters during the day) serve as a principal mechanism of predator avoidance.

Evidence for high predation pressure at Piña is substantial. The locality has yielded numerous predatory shark taxa, including *Otodus megalodon* (Carrillo-Briceño et al., 2015), and

the frequent occurrence of large predatory vertebrates (e.g., dolphins, billfishes) and abundant elasmobranch teeth at the Piña locality (Fierstine, 1978; Vigil & Laurito, 2014; Carrillo-Briceño et al., 2015; Pyenson et al., 2015; De Gracia et al., 2022). Particularly striking, but as yet unremarked, is the extraordinary abundance of cookiecutter shark teeth (*Isistius*). While such teeth have been observed in Neogene tropical American sediments, their frequency at the Piña Chagres site is exceptional (see Table S1). As *Isistius* preferentially parasitizes large marine mammals, fishes, and sharks (Papastamatiou et al., 2010), their abundance testifies to a remarkably high predator density. The Piña scenario parallels tropical upwelling systems in the modern Arabian Sea, where primary production predominantly channels relatively directly into mesopelagic fish communities (Gjøsaeter, 1984). In such ecosystems, primary production is also efficiently transferred through mesopelagic fishes to higher trophic levels, particularly to apex predators.

The combination of strong coastal upwelling, extremely high planktivore abundance, and intense predation pressure thus explains the ecological observations at Piña. The absence of other planktotrophic diurnal taxa further suggests that predation must have been high. The Piña assemblage therefore represents a fossil example of a shallow-water, upwelling-driven, mesopelagic fish-dominated ecosystem during the late Miocene, providing valuable insights into trophic dynamics and ecosystem structure just prior to the final formation of the Isthmus of Panama.

Conclusions

The exceptionally abundant fossil otolith assemblage from the Chagres Formation at Piña reveals an extraordinary dominance of mesopelagic myctophid fishes during the late Miocene in Caribbean Panama. Our otolith collection, based on over 6,200 specimens, consists of 31 taxa belonging to 12 families, and the otolith densities are among the highest ever documented from fossil deposits. Taphonomic observations, including clustered otolith distributions and close associations with ichnofossils, indicate that otoliths entered the sediments mainly through predator-prey interactions, with additional preservation facilitated by burrowing organisms. Although the dominance of mesopelagic taxa typically implies deeper-water settings (Nolf & Brzobohatý, 1992; Lin et al., 2016, 2017, 2018), the co-occurrence of shallow-water taxa and sedimentological evidence (Stiles et al., 2022) indicate deposition in a highly dynamic, shallow-marine environment influenced by coastal upwelling. Our findings reveal previously unrecognized ecological dynamics in ancient tropical coastal ecosystems, where mesopelagic fishes aggregated nearshore in response to nutrient-rich conditions, supporting high populations of apex predators. The Piña assemblage, therefore, represents a rare fossil record of a shallow, mesopelagic fish-dominated ecosystem linked to coastal upwelling during the late Miocene.

Acknowledgements

We thank Brígida De Gracia for assistance with logistics and for facilitating access to relevant fossil collections at the Smithsonian Tropical Research Institute. Fieldwork support was provided

by Blanca Figuerola, Mila O'Dea, Jorge Morales, Katie Griswold, Ramiro J. Solís, Kimberly García-Méndez, Antoni Lombarte, Yehudi Rodriguez Arriatti, Javier Pardo, Laura Lardinois, and Meng-Chen Ko. We are also grateful to Hsin-Wei Liu (Biodiversity Research Center, Academia Sinica, BRCAS) for figure preparation and logistical support, Siao-Man Wu (BRCAS) for assistance with figures, and Chi-Wei Chien for helpful initial discussions on ichnofossils.

References

Agiadi K, Azzarone M, Hua Q, Kaufman DS, Thivaiou D, Albano PG. 2022. The taphonomic clock in fish otoliths. *Paleobiology* 48:154–170.

Aguilera O, Lopes RT, Rodriguez F, dos Santos TM, Rodrigues-Almeida C, Almeida P, Machado AS, Moretti T. 2020. Fossil sea catfish (Siluriformes; Ariidae) otoliths and in-skull otoliths from the Neogene of the Western Central Atlantic. *Journal of South American earth sciences* 101:102619.

Aguilera O, Rodrigues de Aguilera D. 1999. Bathymetric distribution of Miocene to Pleistocene Caribbean teleostean fishes from the coast of Panama and Costa Rica. *Bulletins of American paleontology* 357:251–269.

Aguilera O, Rodrigues de Aguilera D. 2001. An exceptional coastal upwelling fish assemblage in the Caribbean Neogene. *Journal of paleontology* 75:732–742.

Aguilera O, Rodrigues de Aguilera D. 2003. Two new otolith-based sciaenid species of the genus *Plagioscion* from the South American Neogene marine sediments. *Journal of paleontology* 77:1133–1138.

Aguilera O, Schwarzhans W, Béarex P. 2016. Otoliths of the Sciaenidae from the Neogene of tropical America. *Palaeo Ichthyologica* 14:7–90.

Aguilera O, Schwarzhans W, Moraes-Santos H, Nepomuceno A. 2014. Before the flood: Miocene otoliths from eastern Amazon Pirabas Formation reveal a Caribbean-type fish fauna. *Journal of South American Earth Sciences* 56:422–446.

Benites-Palomino A, Vélez-Juarbe J, De Gracia C, Jaramillo C. 2023. Bridging two oceans: small toothed cetaceans (Odontoceti) from the Late Miocene Chagres Formation, eastern Caribbean (Colon, Panama). *Biology letters* 19:20230124.

Brzobohatý R, Nolf D. 2000. *Diaphus* otoliths from the European Neogene (Myctophidae, Teleostei). *Bulletin de l'Institut royal des Sciences naturelles de Belgique, Sciences de la Terre* 70:185–206.

Buchs DM, Irving D, Coombs H, Miranda R, Wang J, Coronado M, Arrocha R, Lacerda M, Goff C, Almengor E, Portugal E, Franceschi P, Chichaco E, Redwood SD. 2019. Volcanic contribution to emergence of Central Panama in the Early Miocene. *Scientific reports* 9:1417.

Cadena E-A, Gracia CD, Combita-Romero DA. 2023. An Upper Miocene marine turtle from Panama that preserves osteocytes with potential DNA. *Journal of vertebrate paleontology* 43. DOI: 10.1080/02724634.2023.2254356.

Carrillo-Briceño JD, De Gracia C, Pimiento C, Aguilera OA, Kindlimann R, Santamarina P, Jaramillo C. 2015. A new Late Miocene chondrichthyan assemblage from the Chagres Formation, Panama. *Journal of South American earth sciences* 60:56–70.

Chao A, Chiu C-H, Jost L. 2014. Unifying species diversity, phylogenetic diversity, functional diversity, and related similarity and differentiation measures through Hill numbers. *Annual review of ecology, evolution, and systematics* 45:297–324.

Chao A, Kubota Y, Zelený D, Chiu C-H, Li C-F, Kusumoto B, Yasuhara M, Thorn S, Wei C-L, Costello MJ, Colwell RK. 2020. Quantifying sample completeness and comparing diversities among assemblages. *Ecological research* 35:292–314.

Chavez FP, Ryan J, Lluch-Cota SE, Niquen C M. 2003. From anchovies to sardines and back: multidecadal change in the Pacific Ocean. *Science (New York, N.Y.)* 299:217–221.

Coates AG. 1999. Lithostratigraphy of the Neogene strata of the Caribbean Coast from Limon, Costa Rica, to Colon, Panama. *Bulletins of American paleontology* 357:17–38.

Coates AG, Obando JA. 1996. The geologic evolution of the Central American Isthmus. In: Jackson JBC, Budd AF, Coates AG eds. *Evolution and Environment in Tropical America*. Chicago: The University of Chicago Press, 21–56.

Collins LS, Aguilera OA, Borne PF, Cairns SD. 1999. A paleoenvironmental analysis of the Neogene of Caribbean Panama and Costa Rica using several phyla. *Bulletins of American paleontology*:81–87.

Collins LS, Coates AG. 1993. Marine paleobiogeography of Caribbean Panama: last Pacific influences before closure of the Tropical American Seaway. *Geological Society of America Annual Meeting, Abstracts with Programs* 25:A–428.

Collins LS, Coates AG, Berggren WA, Aubry M-P, Zhang J. 1996. The late Miocene Panama isthmian strait. *Geology* 24:687.

Conversani VRM, Brenha-Nunes MR, Santificetur C, Giaretta MB, Siliprandi CC, Rossi-Wongtschowski CLDB. 2017. Atlas of marine bony fish otoliths (sagittae) of Southeastern-Southern Brazil Part VII: Atheriniformes, Beloniformes, Beryciformes, Zeiformes, Syngnathiformes, Scorpaeniformes and Tetraodontiformes. *Brazilian journal of oceanography* 65:400–447.

De Gracia C, Correa-Metrio A, Carvalho M, Velez-Juarbe J, Přikryl T, Jaramillo C, Kriwet J. 2022. Towards a unifying systematic scheme of fossil and living billfishes (Teleostei, Istiophoridae). *Journal of systematic palaeontology* 20:1–36.

Farris DW, Jaramillo C, Bayona G, Restrepo-Moreno SA, Montes C, Cardona A, Mora A, Speakman RJ, Glascock MD, Valencia V. 2011. Fracturing of the Panamanian Isthmus during initial collision with South America. *Geology* 39:1007–1010.

Fierstine HL. 1978. A New Marlin, *Makaira panamensis*, from the Late Miocene of Panama. *Copeia* 1978:1.

Fitch JE, Brownell RL Jr. 1968. Fish otoliths in cetacean stomachs and their importance in interpreting feeding habits. *Journal of the Fisheries Research Board of Canada* 25:2561–2575.

Girone A, Nolf D, Cavallo O. 2010. Fish otoliths from the pre-evaporitic (Early Messinian) sediments of northern Italy: their stratigraphic and palaeobiogeographic significance. *Facies* 56:399–432.

GjØsaeter J. 1984. Mesopelagic fish, a large potential resource in the Arabian Sea. *Deep-sea research. Part A, Oceanographic research papers* 31:1019–1035.

Grossman EL, Robbins JA, Rachello-Dolmen PG, Tao K, Saxena D, O'Dea A. 2019. Freshwater input, upwelling, and the evolution of Caribbean coastal ecosystems during formation of the Isthmus of Panama. *Geology* 47:857–861.

Haimovici M, Dos S. Rodrigues L, Lucato SHB, De A. Freire M, Fischer LG, Cardoso LG. 2024. Otolith atlas for marine fishes of the southwestern Atlantic occurring along southern Brazil (28° S-34° S). *Marine and fishery sciences* 37. DOI: 10.47193/mafis.3712024010101.

Hanna CD, Church CC. 1928. Freezing and thawing to disintegrate shales. *Journal Paleontology* 2:131.

Haug GH, Tiedemann R. 1998. Effect of the formation of the Isthmus of Panama on Atlantic Ocean thermohaline circulation. *Nature* 393:673–676.

Hendy AJW. 2013. Spatial and stratigraphic variation of marine paleoenvironments in the middle-upper Miocene Gatun formation, isthmus of panama. *Palaios* 28:210–227.

Herrig E. 1966. Ostracoden aus der Weißen Schreibkreide (Unter-Maastricht) der Insel Rügen. *Paläontologische Abhandlungen* 2:693–1024.

Hill MO. 1973. Diversity and evenness: A unifying notation and its consequences. *Ecology* 54:427–432.

Hsieh TC, Ma KH, Chao A. 2016. iNEXT: an R package for rarefaction and extrapolation of species diversity (Hill numbers). *Methods in ecology and evolution* 7:1451–1456.

Jackson JBC, O'Dea A. 2023. Evolution and environment of Caribbean coastal ecosystems. *Proceedings of the National Academy of Sciences of the United States of America* 120:e2307520120.

Jackson JBC, Todd JA, Fortunato H, Jung P. 1999. Diversity and assemblages of Neogene Caribbean Mollusca of lower Central America. *Bulletins of American paleontology* 357:193–230.

Kordas RL, Pawar S, Kontopoulos D-G, Woodward G, O'Gorman EJ. 2022. Metabolic plasticity can amplify ecosystem responses to global warming. *Nature communications* 13:2161.

Kotlyar AN. 1996. Beryciform Fishes of the World Ocean. VNIRO Publishing, Moscow, 368 pp. [In Russian]

Leonhard I, Agiadi K. 2023. Addressing challenges in marine conservation with fish otoliths and their death assemblages. *Geological Society, London, Special Publications* 529:243–262.

Lin C-H, Brzobohatý R, Nolf D, Girone A. 2017. Tortonian teleost otoliths from northern Italy: taxonomic synthesis and stratigraphic significance. *European journal of taxonomy* 322:1–44.. DOI: 10.5852/ejt.2017.322.

Lin C-H, Chang C-W. 2012. *Otolith Atlas of Taiwan Fishes*. National Museum of Marine Biology & Aquarium.

Lin C-H, Chiang Y-P, Tuset VM, Lombarte A, Girone A. 2018. Late Quaternary to Recent diversity of fish otoliths from the Red Sea, central Mediterranean, and NE Atlantic sea bottoms. *Geobios* 51:335–358. DOI: 10.1016/j.geobios.2018.06.002

Lin C-H, De Gracia B, Pierotti MER, Andrews AH, Griswold K, O'Dea A. 2019. Reconstructing reef fish communities using fish otoliths in coral reef sediments. *PloS one* 14:e0218413.

Lin C-H, Girone A, Nolf D. 2015. Tortonian fish otoliths from turbiditic deposits in northern Italy: taxonomic and stratigraphic significance. *Geobios* 48:249–261. DOI: 10.1016/j.geobios.2015.03.003

Lin C-H, Girone A, Nolf D. 2016. Fish otolith assemblages from Recent NE Atlantic sea bottoms: A comparative study of palaeoecology. *Palaeogeography, Palaeoclimatology, Palaeoecology* 446:98–107. DOI: 10.1016/j.palaeo.2016.01.022

Lin C-H, Lin J-S, Chen K-S, Chen M-H, Chen C-Y, Chang C-W. 2020. Feeding habits of bigeye tuna (*Thunnus obesus*) in the western Indian ocean reveal a size-related shift in its fine-scale piscivorous diet. *Frontiers in marine science* 7:582571. DOI: 10.3389/fmars.2020.582571.

Lin C-H, Taviani M, Angeletti L, Girone A, Nolf D. 2017. Fish otoliths in superficial sediments of the Mediterranean Sea. *Palaeogeography, Palaeoclimatology, Palaeoecology* 471:134–143. DOI: 10.1016/j.palaeo.2016.12.050

Lin C-H, Wei C-L, Ho SL, Lo L. 2023a. Ocean temperature drove changes in the mesopelagic fish community at the edge of the Pacific Warm Pool over the past 460,000 years. *Science advances* 9:eadf0656. DOI: 10.1126/sciadv.adf0656

Lin C-H, Wu S-M, Lin C-Y, Chien C-W. 2023b. Early Pliocene otolith assemblages from the outer-shelf environment reveal the establishment of mesopelagic fish fauna over 3 million years ago in southwestern Taiwan. *Swiss Journal of Palaeontology* 142:23.

Martin R, Dunn D. 2000. Otoliths of the Late Miocene Gatun Formation of Panama. *Gulf Coast Association of Geological Societies Transactions* 50:687–696.

Martin RP, Olson EE, Girard MG, Smith WL, Davis MP. 2018. Light in the darkness: New perspective on lanternfish relationships and classification using genomic and morphological data. *Molecular phylogenetics and evolution* 121:71–85.

Nelson JS, Grande TC, Wilson MVH. 2016. *Fishes of the world*. John Wiley & Sons.

Ng S-L, Lin C-H, Liu K-M, Joung S-J. 2024a. New records of three mesopelagic fish species from southwestern Taiwan. *Thalassas: An International Journal of Marine Sciences* 40:81–90.

Ng S-L, Liu K-M, Joung S-J. 2023. *Malakichthys formosus*, a new species of small seabass (Acropomatiformes: Malakichthyidae) from southwestern Taiwan. *Zootaxa* 5380:380–386.

Ng S-L, Liu H-W, Mediodia DP, Lin Y-T, Lee C-H, Lin C-F, Huang S-P, Wu S-M, Tung C-R, Ho H-C, Lin C-H. 2024b. An updated checklist of fishes of Dongsha Island, Taiwan, northern South China Sea. *ZooKeys* 1220:175–242.

912 Nolf D. 1976. Les otoliths des Téléostéens néogènes de Trinidad. *Eclogae Geologicae Helvetiae*
913 69:703–742.
914 Nolf D. 1985. *Otolithi piscium*. Fischer, Stuttgart, New York.
915 Nolf D. 2013. The diversity of fish otoliths, past and present.
916 Nolf D, Aguilera O. 1998. Fish otoliths from the Cantaure Formation (Early Miocene of
917 Venezuela). *Bulletin de l'Institut royal des Sciences naturelles de Belgique, Sciences de la*
918 *Terre* 68:237–262.
919 Nolf D, Brzobohatý R. 1992. Fish otoliths as paleobathymetric indicators. *Paleontologia i*
920 *Evolucio* 24–25:255–264.
921 Nolf D, Steurbaut E. 1983. Révision des otolithes de téléostéens du Tortonien stratotypique et de
922 Montegibbio (Miocène Supérieur d'Italie septentrionale). *Mededelingen van de Werkgroep*
923 *voor Tertiaire en Kwartaire Geologie* 20:143–197.
924 Nolf D, Stringer GL. 1992. Neogene paleontology in the northern Dominican Republic. *Bulletins*
925 *of American paleontology* 102:41–81.
926 O'Dea A, Jackson J, Fortunato H, Smith T, Croz D, Kg Todd J. 2007. Environmental change
927 preceded Caribbean mass extinction by 2 million years. *Proceedings of the National*
928 *Academy of Sciences* 104:5501–5506.
929 O'Dea A, Lessios HA, Coates AG, Eytan RI, Restrepo-Moreno SA, Cione AL, Collins LS, de
930 Queiroz A, Farris DW, Norris RD, Stallard RF, Woodburne MO, Aguilera O, Aubry M-P,
931 Berggren WA, Budd AF, Cozzuol MA, Coppard SE, Duque-Caro H, Finnegan S, Gasparini
932 GM, Grossman EL, Johnson KG, Keigwin LD, Knowlton N, Leigh EG, Leonard-Pingel JS,
933 Marko PB, Pyenson ND, Rachello-Dolmen PG, Soibelzon E, Soibelzon L, Todd JA,
934 Vermeij GJ, Jackson JBC. 2016. Formation of the isthmus of Panama. *Science advances*
935 2:e1600883.
936 Papastamatiou YP, Wetherbee BM, O'Sullivan J, Goodmanlowe GD, Lowe CG. 2010. Foraging
937 ecology of Cookiecutter Sharks (*Isistius brasiliensis*) on pelagic fishes in Hawaii, inferred
938 from prey bite wounds. *Environmental biology of fishes* 88:361–368.
939 Pyenson ND, Vélez-Juarbe J, Gutstein CS, Little H, Vigil D, O'Dea A. 2015. *Isthminia*
940 *panamensis*, a new fossil inioid (Mammalia, Cetacea) from the Chagres Formation of
941 Panama and the evolution of "river dolphins" in the Americas. *PeerJ* 3:e1227.
942 Rivaton J, Bourret P. 1999. *Les otolithes des poissons de l'Indo-Pacifique*. Institut de recherche
943 pour le développement.
944 Schubert RJ. 1908. Fischreste. In: Toula F ed. *Eine jungtertiäre Faunavon Gatun am Panama-*
945 *Kanal*. Jb. k.k. Geol. Reichsanst., 687–691.
946 Schwarzhans W. 2013. A comparative morphological study of the Recent otoliths of the genera
947 *Diaphus*, *Idiolychnus* and *Lobianchia* (Myctophidae). *Palaeo Ichthyologica* 13:41–82.
948 Schwarzhans W. 2019. A comparative morphological study of Recent otoliths of the Congridae,
949 Muraenesocidae, Nettastomatidae and Colocongridae (Anguilliformes). *Memorie della*
950 *società Italiana di scienze naturali e del museo di storia naturale di Milano* 46:327–354.

Schwarzhans W, Aguilera O. 2013. Otoliths of the Myctophidae from the Neogene of tropical America. *Palaeo Ichthyologica* 13:83–150.
Schwarzhans W, Aguilera O. 2016. Otoliths of the Ophidiiformes from the Neogene of tropical America. *Palaeo Ichthyologica* 14:91–124.
Schwarzhans WW, Aguilera OA. 2024. Otoliths of the Gobiidae from the Neogene of tropical America. *Swiss Journal of Palaeontology* 143:13.
Schwarzhans W, Milàn J., Carnevale G. 2021. A tale from the middle Paleocene of Denmark: A tube-dwelling predator documented by the ichnofossil *Lepidenteron mortenseni* n. isp. and its predominant prey, *Bobbitichthys* n. gen. *rosenkrantzi* (Macrouridae, Teleostei). *Bulletin of the Geological Society of Denmark* 69:35–52.
Schwarzhans W, Nielsen S. 2021. Fish otoliths from the early Miocene of Chile: a window into the evolution of marine bony fishes in the Southeast Pacific. *Swiss journal of palaeontology* 140. DOI: 10.1186/s13358-021-00228-w.
Schwarzhans W, Ohe F, Tsuchiya Y, Ujihara A. 2022. Lanternfish otoliths (Myctophidae, Teleostei) from the Miocene of Japan. *Zitteliana* 96:103–134.
Schwarzhans WW, Prokofiev AM. 2017. Reappraisal of *Synagrops* Günther, 1887 with rehabilitation and revision of *Parascombrops* Alcock, 1889 including description of seven new species and two new genera (Perciformes: Acropomatidae). *Zootaxa* 4260:1–74.
Stiles E, Montes C, Jaramillo C, Gingras MK. 2022. A shallow-water depositional interpretation for the upper Miocene Chagres Formation (Caribbean coast of Panama). *Geological Society of America bulletin*. DOI: 10.1130/b36291.1.
Stringer G. 1998. Otolith-based fishes from the Bowden shell bed (Pliocene) of Jamaica: systematics and palaeoecology. *Contributions to Tertiary and Quaternary Geology* 35:147–160.
Titus BM, Gibbs HL, Simões N, Daly M. 2024. Topology testing and demographic modeling illuminate a novel speciation pathway in the Greater Caribbean sea following the formation of the Isthmus of Panama. *Systematic biology* 73:758–768.
Velez-Juarbe J, Wood AR, De Gracia C, Hendy AJW. 2015. Evolutionary patterns among living and fossil kogiid sperm whales: Evidence from the Neogene of central America. *PloS one* 10:e0123909.
Vigil DI, Laurito CA. 2014. Nuevos restos de un Odontoceti fósil (Mammalia: Cetacea, Physeteroidea) para el Mioceno Tardío de Panamá, América Central. *Revista geológica de América central*. DOI: 10.15517/rgac.v0i50.15123.
Woodring WP. 1957. Geology and paleontology of Canal Zone and adjoining parts of Panama. *U.S. Geological Survey Professional Paper* 306A:145.
Yamanoue Y, Matsuura K. 2004. A review of the genus *Malakichthys* Döderlein (Perciformes: Acropomatidae) with the description of a new species. *Journal of fish biology* 65:511–529.

Figures

Figure 1. Sampling site and geological map. Figure modified after Collins et al. (1996) and Carrillo-Briceño et al. (2015).

Figure 2. Lithostratigraphy (A, modified after Carrillo-Briceño et al. 2015; Stiles et al. 2022) and photographs of the site (B–D). (C and D) Abundant fish otoliths and associated ichnofossil *Ophiomorpha* are visible on the surface of the outcrop. Red arrow = sampling layer.

Figure 3. Otoliths of Congridae and Argentinidae from the late Miocene Chagres Formation, Caribbean Panama. (A and B) *Chiloconger aflorens* sp. nov., (A) holotype, ASIZF 0100943, (B) paratype, ASIZF 0100944. (C) *Rhynchoconger* sp., ASIZF 0100945. (D) *Argentina* sp., ASIZF 0100946. Images are inner views unless otherwise indicated. 1, ventral view; 2, inner view. Scale bar = 1 mm.

Figure 4. Otoliths of Sternoptychidae and Myctophidae from the late Miocene Chagres Formation, Caribbean Panama. (A and B) *Polyipnus* sp., ASIZF 0100947–0948. (C) *Benthosema pluridens* Schwarzhans & Aguliera, 2013, ASIZF 0100949. (D) *Bolinichthys* sp., ASIZF 0100950. Images are inner views. Scale bar = 1 mm.

Figure 5. Otoliths of *Dasyscopelus* (Myctophidae) from the late Miocene Chagres Formation, Caribbean Panama. (A–F) *Dasyscopelus degraciai* (Schwarzhans & Aguliera, 2013), ASIZF 0100951–0956. (G–L) *Dasyscopelus inopinatus* sp. nov., (G, H, J–L) paratypes, ASIZF 0100957–0961, (I) holotype, ASIZF 0100962. Images are inner views unless otherwise indicated. 1, ventral view; 2, inner view. Scale bar = 1 mm.

Figure 6. Otoliths of *Diaphus* (Myctophidae) from the late Miocene Chagres Formation, Caribbean Panama. (A–C) *Diaphus aequalis* Schwarzhans & Aguliera, 2013, ASIZF 0100963–0965. (D–F) *Diaphus apalus* Schwarzhans & Aguliera, 2013, ASIZF 0100966–0968. (G–K) *Diaphus barrigonensis* Schwarzhans & Aguliera, 2013, ASIZF 0100969–0973. (L–O) *Diaphus dumerilii* (Bleeker, 1856), ASIZF 0100974–0977. Images are inner views. Scale bar = 1 mm.

Figure 7. Otoliths of *Diaphus* and *Diogenichthys* (Myctophidae) from the late Miocene Chagres Formation, Caribbean Panama. (A and B) *Diaphus multiserratus* Schwarzhans & Aguliera, 2013, ASIZF 0100978–0979. (C–F) *Diaphus pedemontanus* (Robba, 1970), ASIZF 0100980–0983. (G–J) *Diaphus rodriguezi* Schwarzhans & Aguliera, 2013, ASIZF 0100984–0987. (K) *Diogenichthys* sp., ASIZF 0100988. Images are inner views unless otherwise indicated. 1, ventral view; 2, inner view. Scale bar = 1 mm.

Figure 8. Otoliths of *Lepidophanes*, *Lobianchiaand*, and *Myctophum* (Myctophidae) from the late Miocene Chagres Formation, Caribbean Panama. (A–C) *Lobianchia johnfitchi* Schwarzhans & Aguliera, 2013, ASIZF 0100992–0994. (D–F) *Myctophum arcanum*

Schwarzhans & Aguliera, 2013, ASIZF 0100995–0997. (G and H) *Myctophum affine* (Lütken, 1892), 2013, ASIZF 0100998–0999. (I) *Lepidophanes inflectus* Schwarzhans & Aguliera, 2013, ASIZF 0101000. Images are inner views unless otherwise indicated. 1, ventral view; 2, inner view. Scale bar = 1 mm.

Figure 9. Otoliths of Macrouridae and Bregmacerotidae from the late Miocene Chagres Formation, Caribbean Panama. (A and B) *Coelorinchus* sp., ASIZF 0101001–1002. (C–E) *Bregmaceros* sp., ASIZF 0101003–1005. Images are inner views. Scale bar = 1 mm.

Figure 10. Otoliths of Trachichthyidae, Carapidae, and Ophidiidae from the late Miocene Chagres Formation, Caribbean Panama. (A–D) *Hoplostethus boyae* sp. nov., (A) holotype, ASIZF 0101006, (B–D) paratypes, ASIZF 0101007–1009. (E and F) *Carapus* sp., ASIZF 0101010–1011. (G) *Lepophidium limulum* Schwarzhans & Aguliera, 2013, ASIZF 0101012. Images are inner views unless otherwise indicated. 1, ventral view; 2, inner view. Scale bar = 1 mm.

Figure 11. Otoliths of Opistognathidae and Carangidae from the late Miocene Chagres Formation, Caribbean Panama. (A) *Opistognathus* sp., ASIZF 0101013. (B) Carangidae indet., ASIZF 0101014. 1, ventral view; 2, inner view. Scale bar = 1 mm.

Figure 12. Otoliths of *Malakichthys* (Malakichthyidae) from the late Miocene Chagres Formation, Caribbean Panama. (A–F) *Malakichthys schwarzhansi* sp. nov., (A) holotype, ASIZF 0101015, (B–F) paratypes, ASIZF 0101016–1020. Images are inner views unless otherwise indicated. 1, ventral view; 2, inner view. Scale bar = 1 mm.

Figure 13. Extant *Malakichthys* (Malakichthyidae) otoliths. (A and B) *Malakichthys wakiyae* Jordan & Hubbs, 1925, (A) 86.1 mm SL, CHLOL 10514, (B) 61.4 mm SL, CHLOL 10493. (C and D) *Malakichthys griseus* Döderlein, 1883, (C) 93.7 mm SL, CHLOL 14678, (D) 102.5 mm SL, CHLOL 34344. (E–G) *Malakichthys elegans* Matsubara & Yamaguti, 1943, (E) 131.9 mm SL, CHLOL 8241, (F) 62.9 mm SL, CHLOL 8800, (G) 77.8 mm SL, CHLOL 2605. (H and I) *Malakichthys formosus* Ng, Liu & Joung, 2023, (H) 72.1 mm SL, CHLOL 27488, (I) 64.9 mm SL, CHLOL 31419. (J–L) *Malakichthys barbatus* Yamanoue & Yoseda, 2001, (J) 161.0 mm SL, CHLOL 27489, (K) 83.51 mm SL, CHLOL 35072, (L) 223.5 mm SL, CHLOL 33087. Images are inner views unless otherwise indicated. 1, ventral view; 2, inner view. Scale bar = 1 mm.

Figure 14. Extant *Ambassis* (Ambassidae) otoliths. (A) *Ambassis kopsii* Bleeker, 1858, 69.8 mm SL, CHLOL 28447. (B and C) *Ambassis miops* Günther, 1872, (B) 22.7 mm SL, CHLOL 31077, (C) 22.3 mm SL, CHLOL 31078. (D and E) *Ambassis urotaenia* Bleeker 1852, 1943, (D) 46.8 mm SL, CHLOL 27116, (E) 34.1 mm SL, CHLOL 27115. (F and G) *Ambassis interrupta*

Bleeker, 1853, (F) 34.6 mm SL, CHLOL 27119, (G) 47.8 mm SL, CHLOL 27120. Images are inner views unless otherwise indicated. 1, ventral view; 2, inner view. Scale bar = 1 mm.

Figure 15. Rank abundance of otolith families. Note that y-axis is log-scaled, and the otolith counts are indicated in parentheses.

Figure 16. Rarefaction curves of otolith-based taxa (Hill numbers) represented by species richness (${}^0D$), Shannon diversity (${}^1D$), and Simpson (${}^2D$) diversity. Shaded areas represent 95% confidence intervals based on 1000 bootstrap replicates.

Table

Table 1. List of otolith-based fish taxa from the late Miocene Chagres Formation, Caribbean Panama.

Supplemental files

Table S1. Densities of fish otoliths and *Isistius* teeth from the late Miocene Chagres Formation, Caribbean Panama.

Figure 1

Figure 1. Sampling site and geological map.

Figure modified after Collins et al. (1996) and Carrillo-Briceño et al. (2015).

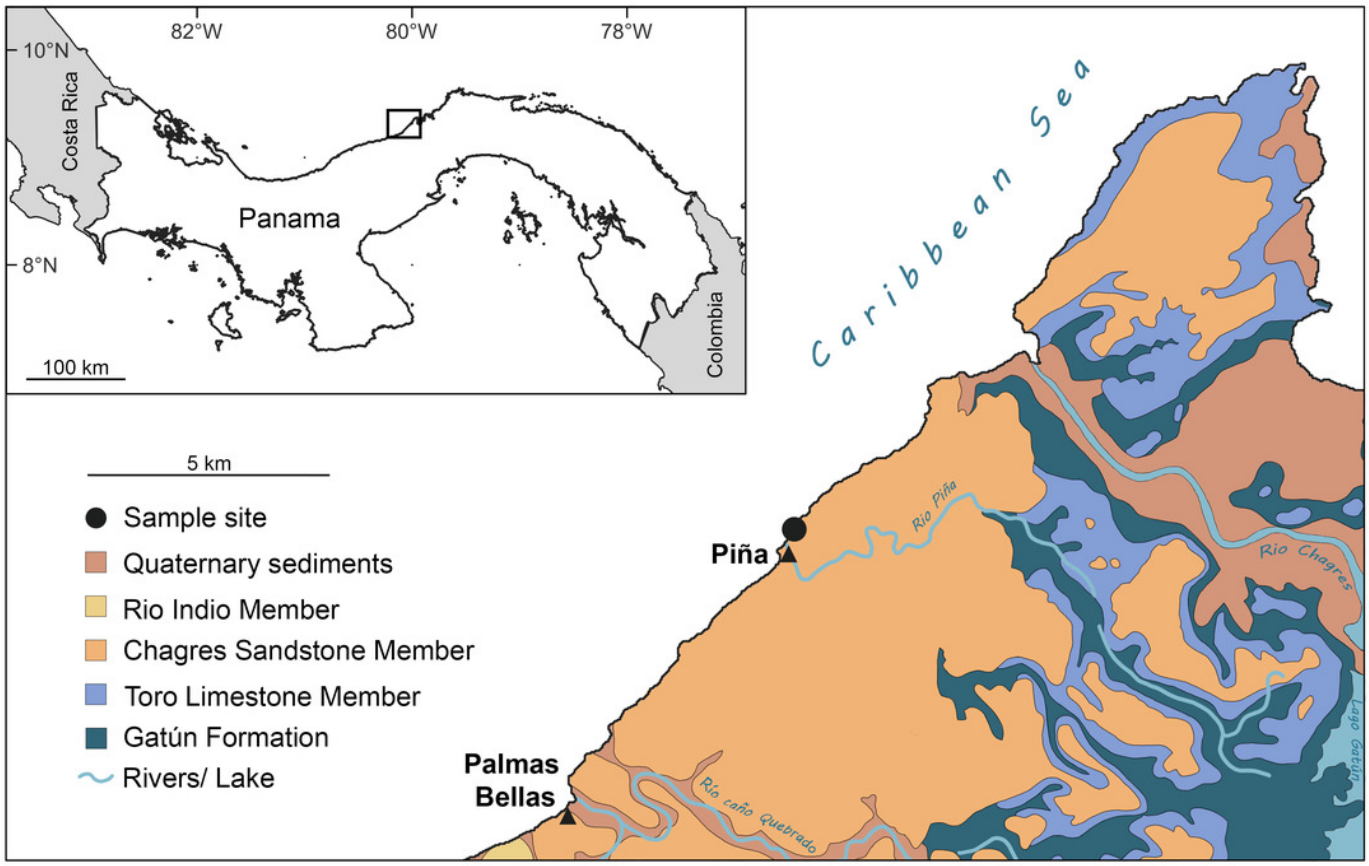

Figure 2

Figure 2. Lithostratigraphy (A, modified after Carrillo-Briceño et al. 2015; Stiles et al. 2022) and photographs of the site (B–D).

(C and D) Abundant fish otoliths and associated ichnofossil *Ophiomorpha* are visible on the surface of the outcrop. Red arrow = sampling layer.

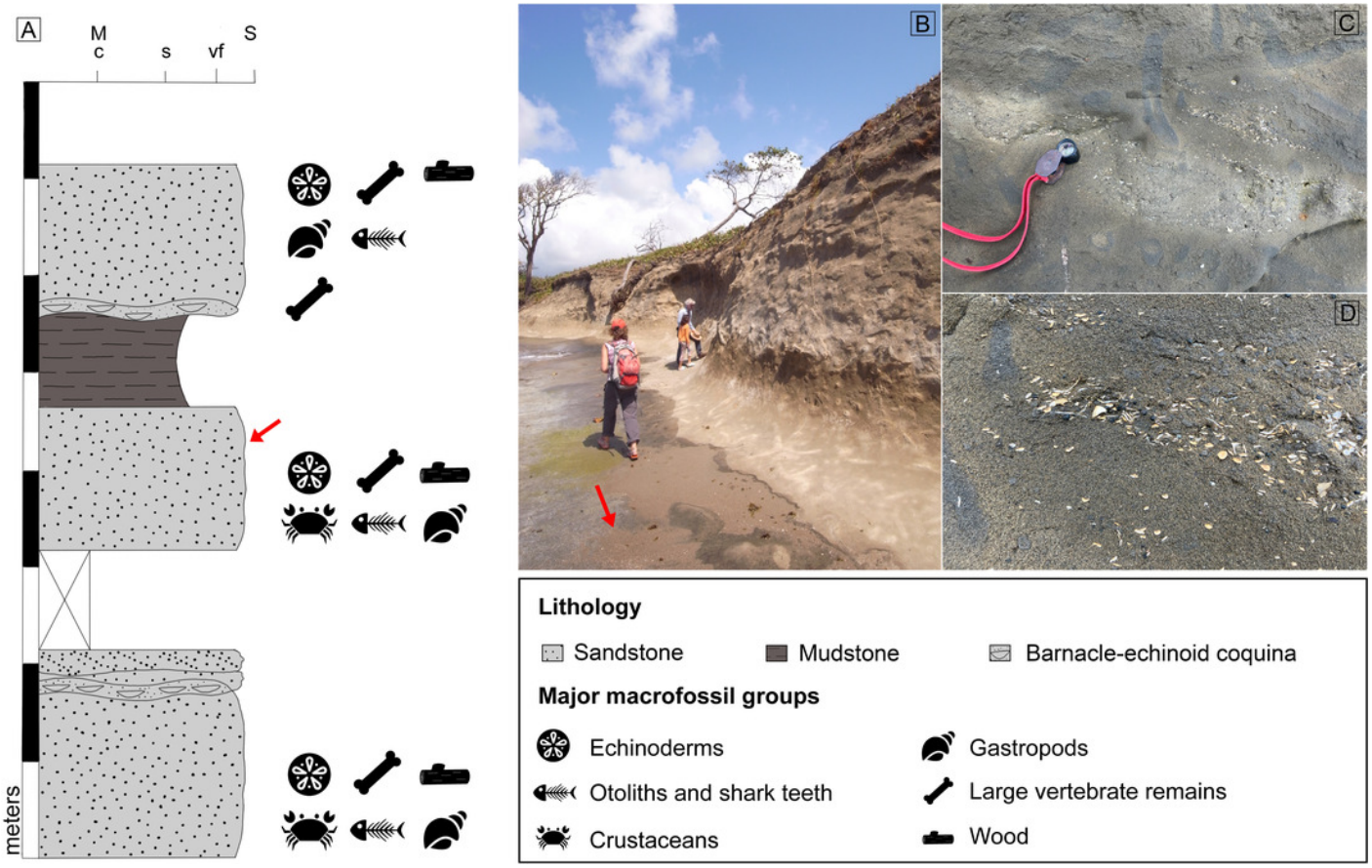

Figure 3

Figure 3. Otoliths of Congridae and Argentinidae from the late Miocene Chagres Formation, Caribbean Panama.

(A and B) *Chiloconger aflorens* sp. nov., (A) holotype, ASIZF 0100943, (B) paratype, ASIZF 0100944. (C) *Rhynchoconger* sp., ASIZF 0100945. (D) *Argentina* sp., ASIZF 0100946. Images are inner views unless otherwise indicated. 1, ventral view; 2, inner view. Scale bar = 1 mm.

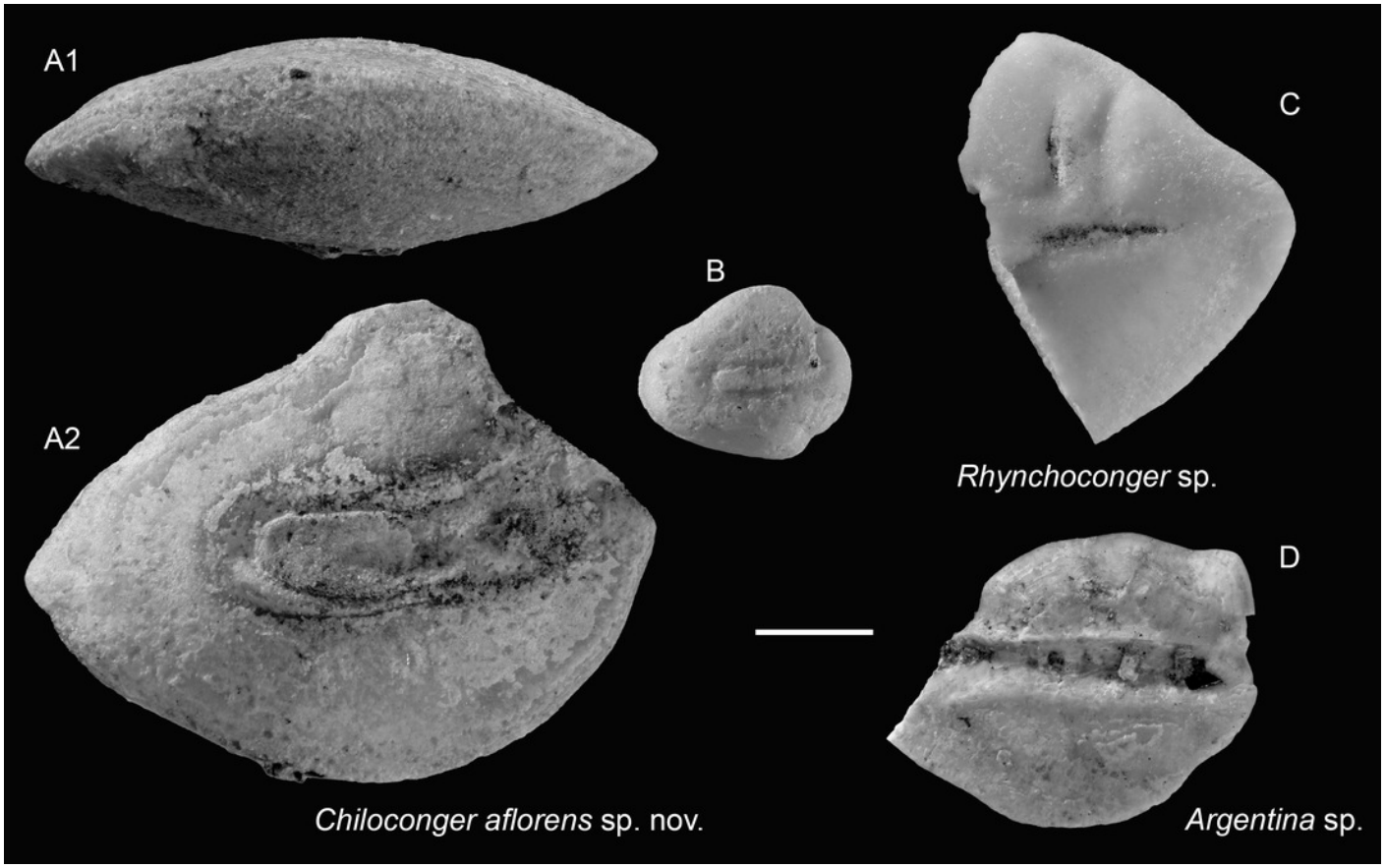

Figure 4

Figure 4. Otoliths of Sternoptychidae and Myctophidae from the late Miocene Chagres Formation, Caribbean Panama.

(A and B) *Polyipnus* sp., ASIZF 0100947–0948. (C) *Benthosema pluridens* Schwarzhans & Aguliera, 2013, ASIZF 0100949. (D) *Bolinichthys* sp., ASIZF 0100950. Images are inner views. Scale bar = 1 mm.

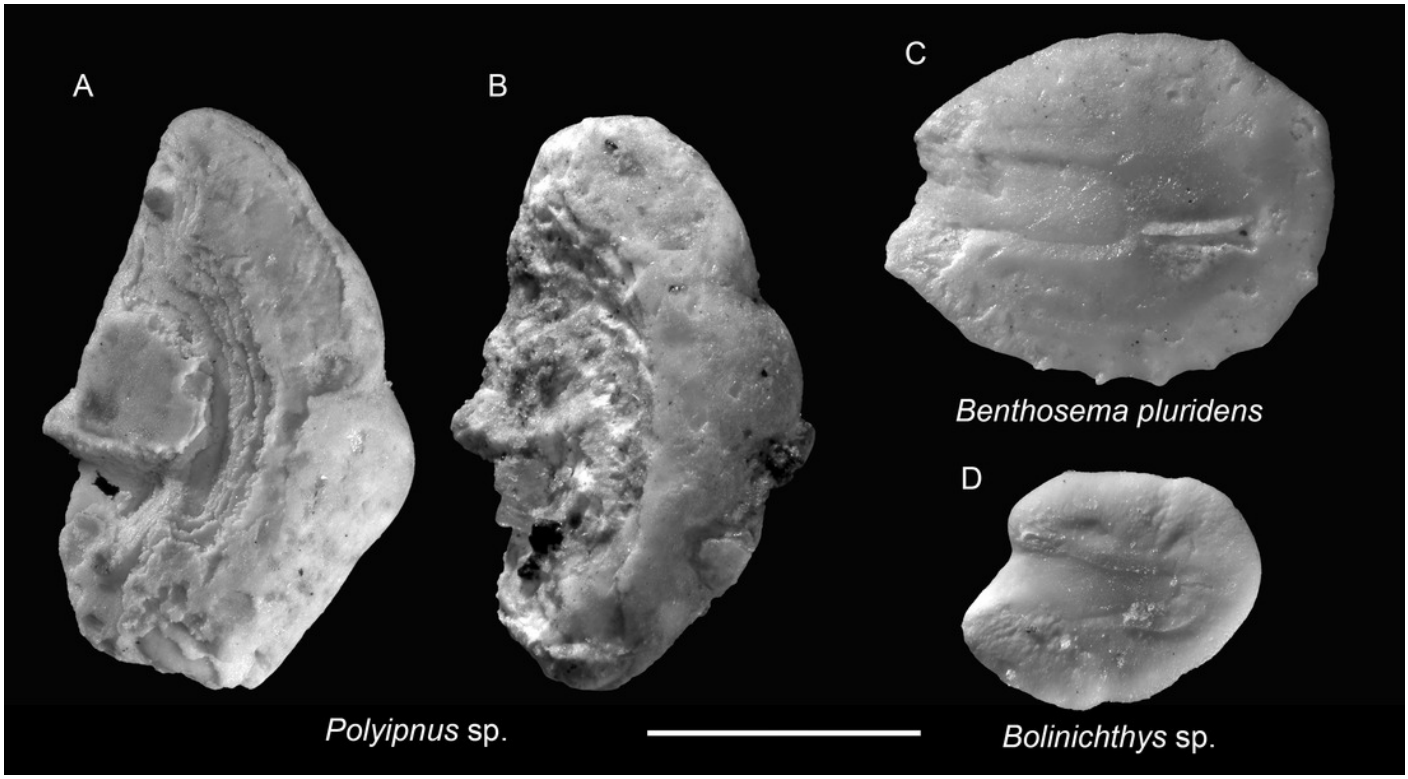

Figure 5

Figure 5. Otoliths of *Dasyscopelus* (Myctophidae) from the late Miocene Chagres Formation, Caribbean Panama.

(A–F) *Dasyscopelus degraciai* (Schwarzhans & Aguliera, 2013), ASIZF 0100951–0956. (G–L) *Dasyscopelus inopinatus* sp. nov., (G, H, J–L) paratypes, ASIZF 0100957–0961, (I) holotype, ASIZF 0100962. Images are inner views unless otherwise indicated. 1, ventral view; 2, inner view. Scale bar = 1 mm.

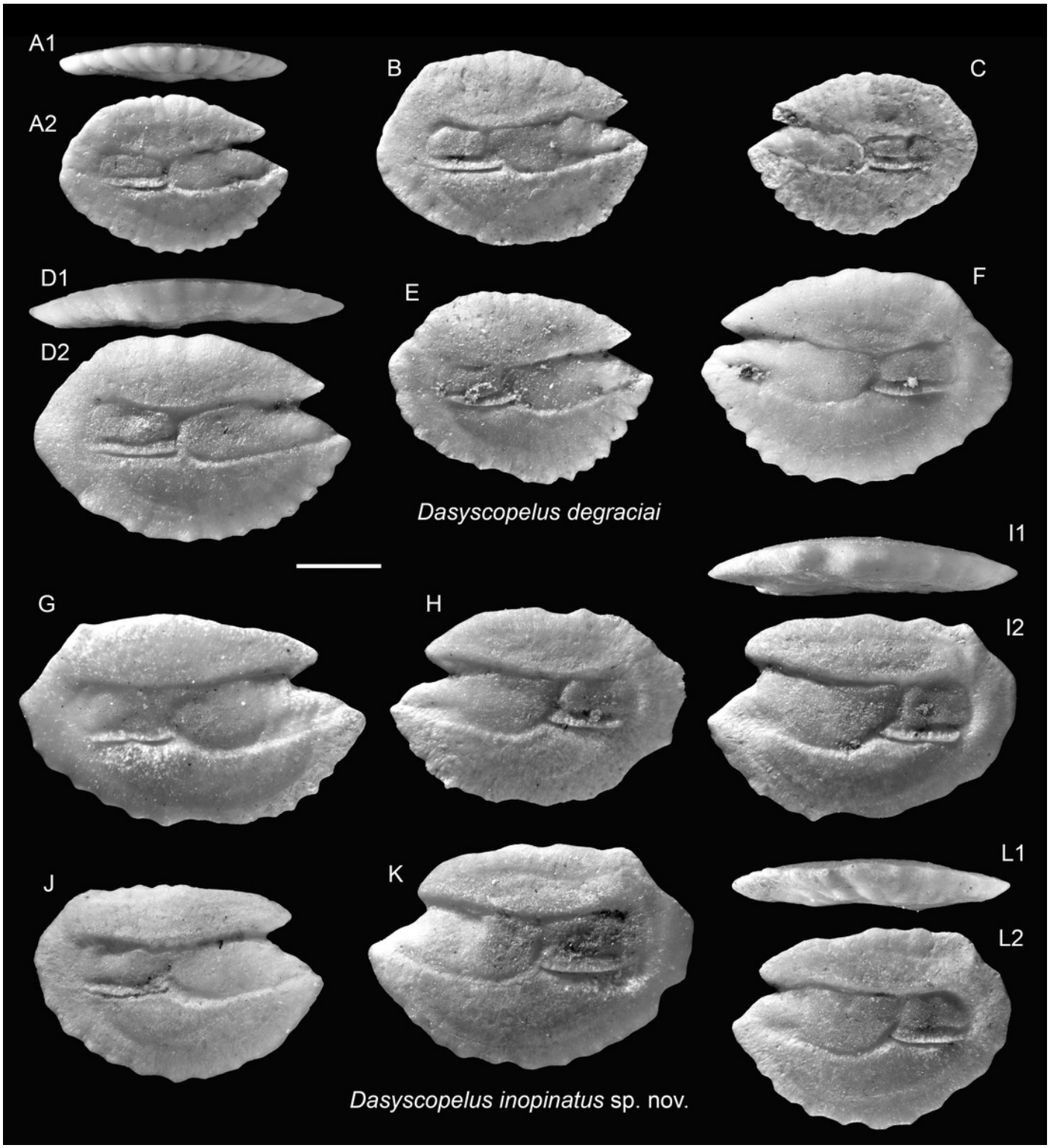
A1
A2
B
C
D1
D2
E
F
Dasyscopelus degraciai
I1
I2
G
H
J
K
L1
L2
Dasyscopelus inopinatus sp. nov.

Figure 6

Figure 6. Otoliths of *Diaphus* (Myctophidae) from the late Miocene Chagres Formation, Caribbean Panama.

(A–C) *Diaphus aequalis* Schwarzhans & Aguliera, 2013, ASIZF 0100963–0965. (D–F) *Diaphus apalus* Schwarzhans & Aguliera, 2013, ASIZF 0100966–0968. (G–K) *Diaphus barrigonensis* Schwarzhans & Aguliera, 2013, ASIZF 0100969–0973. (L–O) *Diaphus dumerilii* (Bleeker, 1856), ASIZF 0100974–0977. Images are inner views. Scale bar = 1 mm.

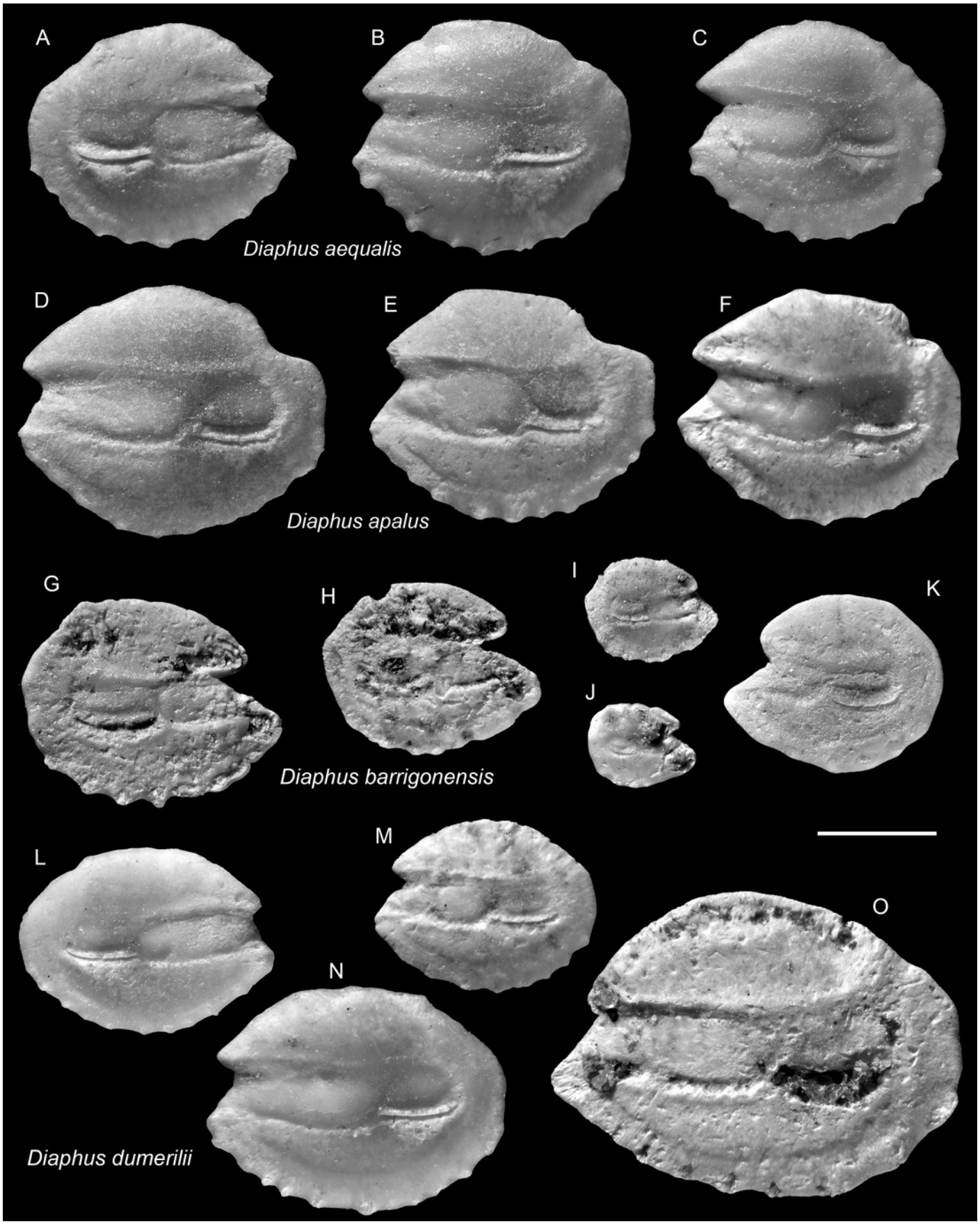
A
B
C
Diaphus aequalis
D
E
F
Diaphus apalus
G
H
I
K
J
Diaphus barrigonensis
L
M
O
N
Diaphus dumerilii

Figure 7

Figure 7. Otoliths of *Diaphus* and *Diogenichthys* (Myctophidae) from the late Miocene Chagres Formation, Caribbean Panama.

(A and B) *Diaphus multiserratus* Schwarzhans & Aguliera, 2013, ASIZF 0100978–0979. (C–F) *Diaphus pedemontanus* (Robba, 1970), ASIZF 0100980–0983. (G–J) *Diaphus rodriguezi* Schwarzhans & Aguliera, 2013, ASIZF 0100984–0987. (K) *Diogenichthys* sp., ASIZF 0100988. Images are inner views unless otherwise indicated. 1, ventral view; 2, inner view. Scale bar = 1 mm.

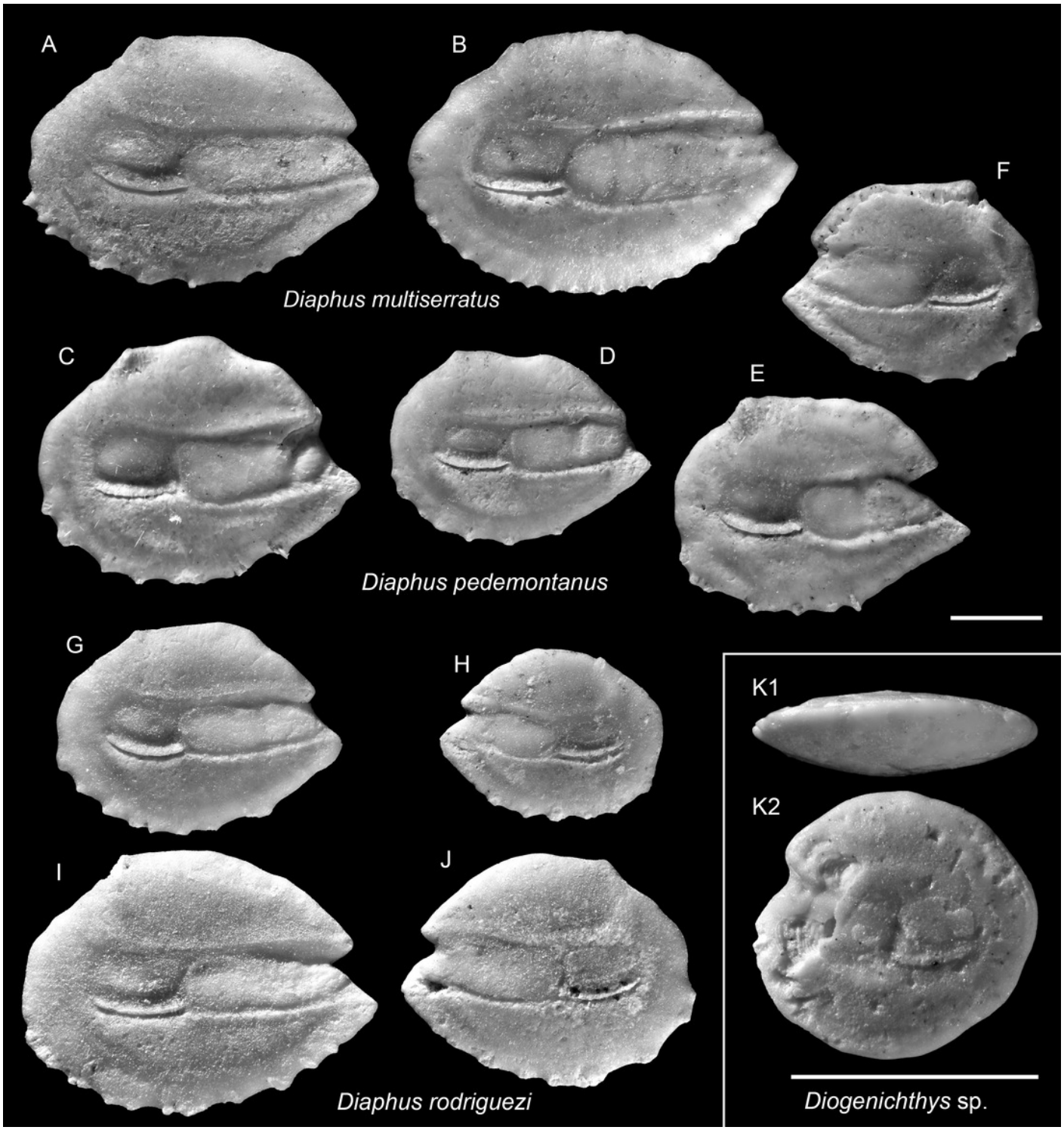
A
B
F
Diaphus multiserratus
C
D
E
Diaphus pedemontanus
G
H
I
J
Diaphus rodriguezi
K1
K2
Diogenichthys sp.

Figure 8

Figure 8. Otoliths of *Lepidophanes*, *Lobianchiaand*, and *Myctophum* (Myctophidae) from the late Miocene Chagres Formation, Caribbean Panama.

(A–C) *Lobianchia johnfitchi* Schwarzhans & Aguliera, 2013, ASIZF 0100992–0994. (D–F) *Myctophum arcanum* Schwarzhans & Aguliera, 2013, ASIZF 0100995–0997. (G and H) *Myctophum affine* (Lütken, 1892), 2013, ASIZF 0100998–0999. (I) *Lepidophanes inflectus* Schwarzhans & Aguliera, 2013, ASIZF 0101000. Images are inner views unless otherwise indicated. 1, ventral view; 2, inner view. Scale bar = 1 mm.

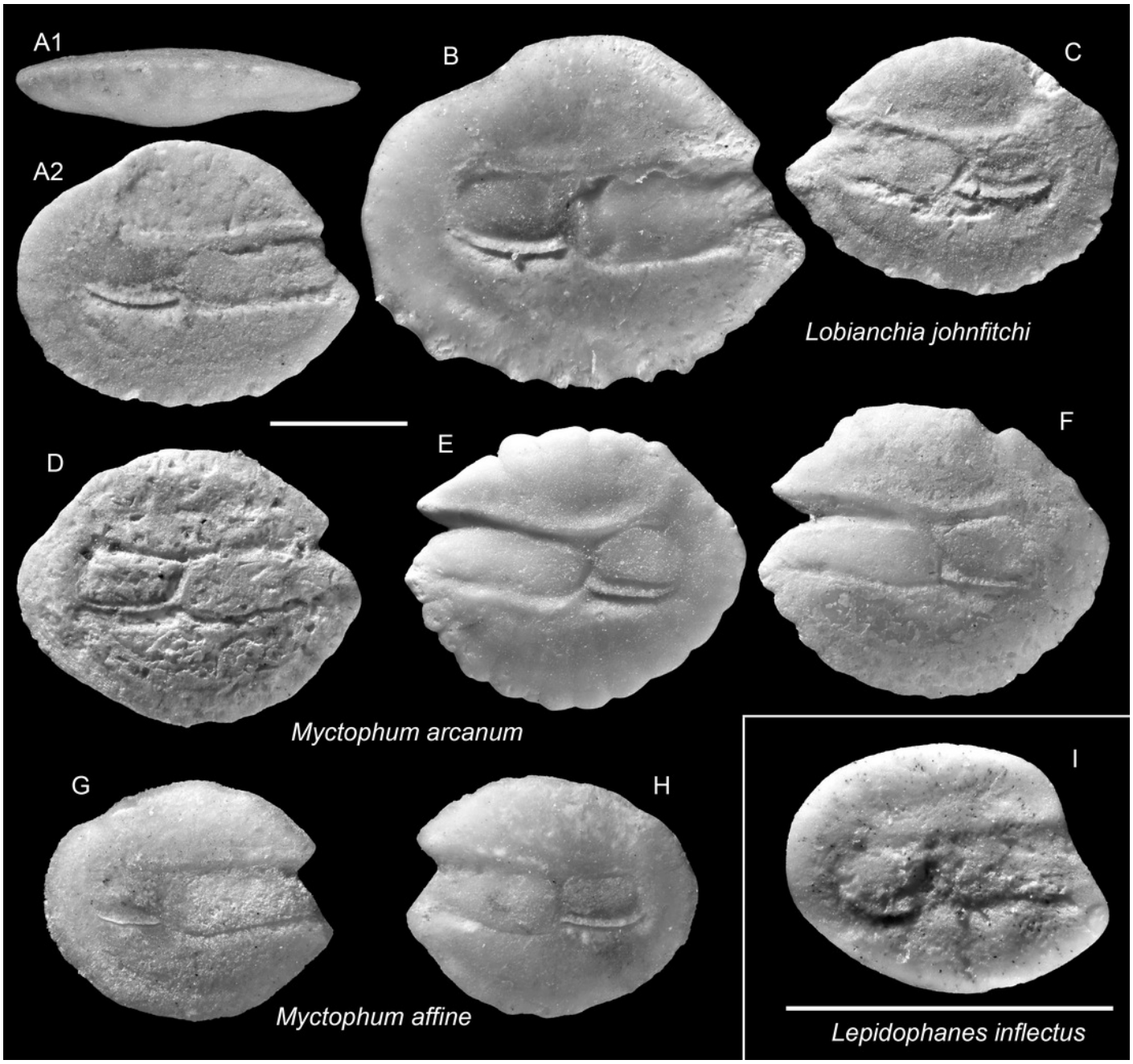
A1
A2
B
C
Lobianchia johnfitchi
D
E
F
Myctophum arcanum
G
H
Myctophum affine
I
Lepidophanes inflectus

Figure 9

Figure 9. Otoliths of Macrouridae and Bregmacerotidae from the late Miocene Chagres Formation, Caribbean Panama.

(A and B) *Coelorinchus* sp., ASIZF 0101001–1002. (C–E) *Bregmaceros* sp., ASIZF 0101003–1005. Images are inner views. Scale bar = 1 mm.

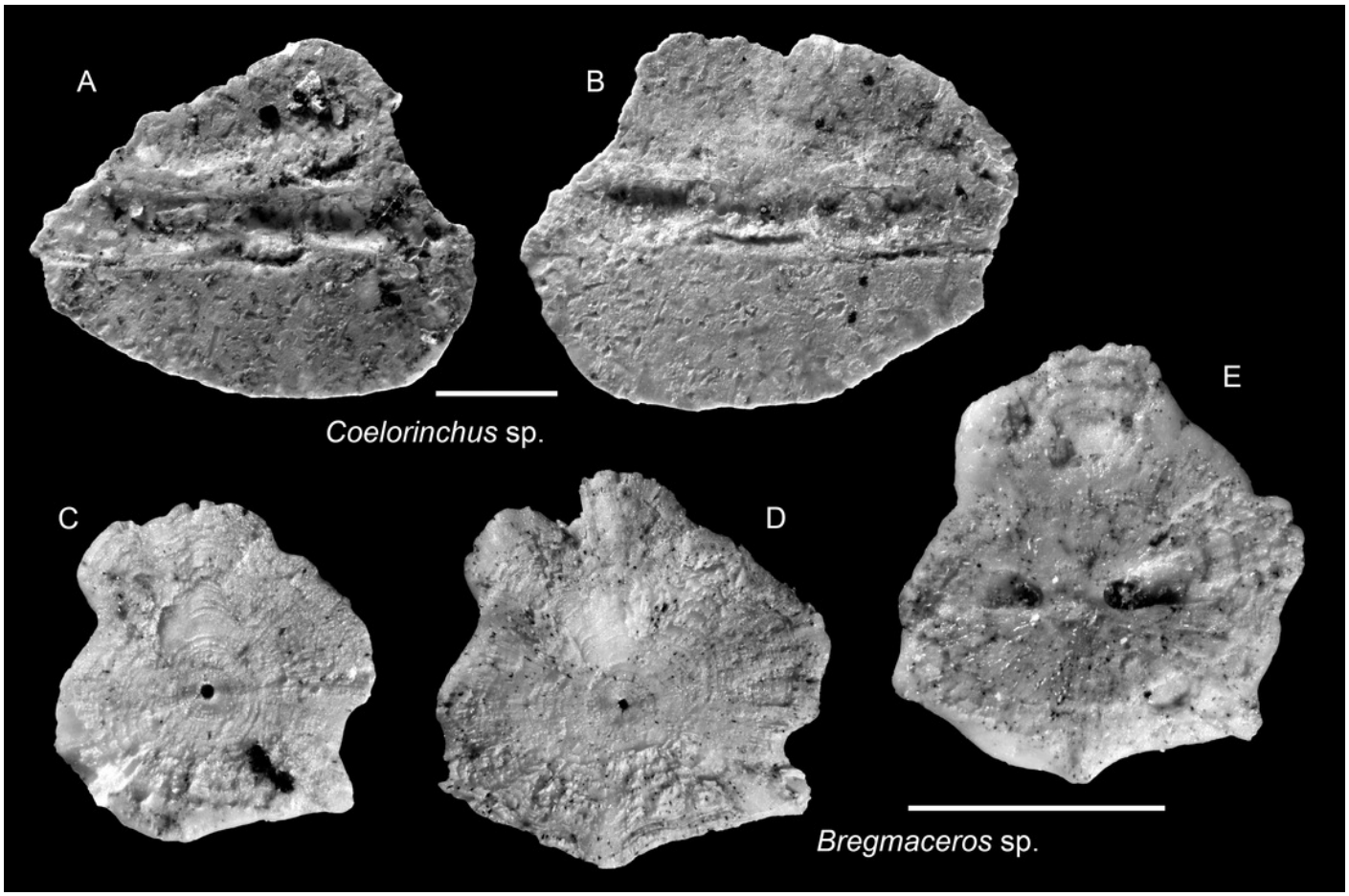

Figure 10

Figure 10. Otoliths of Trachichthyidae, Carapidae, and Ophidiidae from the late Miocene Chagres Formation, Caribbean Panama.

(A–D) *Hoplostethus boyae* sp. nov., (A) holotype, ASIZF 0101006, (B–D) paratypes, ASIZF 0101007–1009. (E and F) *Carapus* sp., ASIZF 0101010–1011. (G) *Lepophidium limulum* Schwarzhans & Aguliera, 2013, ASIZF 0101012. Images are inner views unless otherwise indicated. 1, ventral view; 2, inner view. Scale bar = 1 mm.

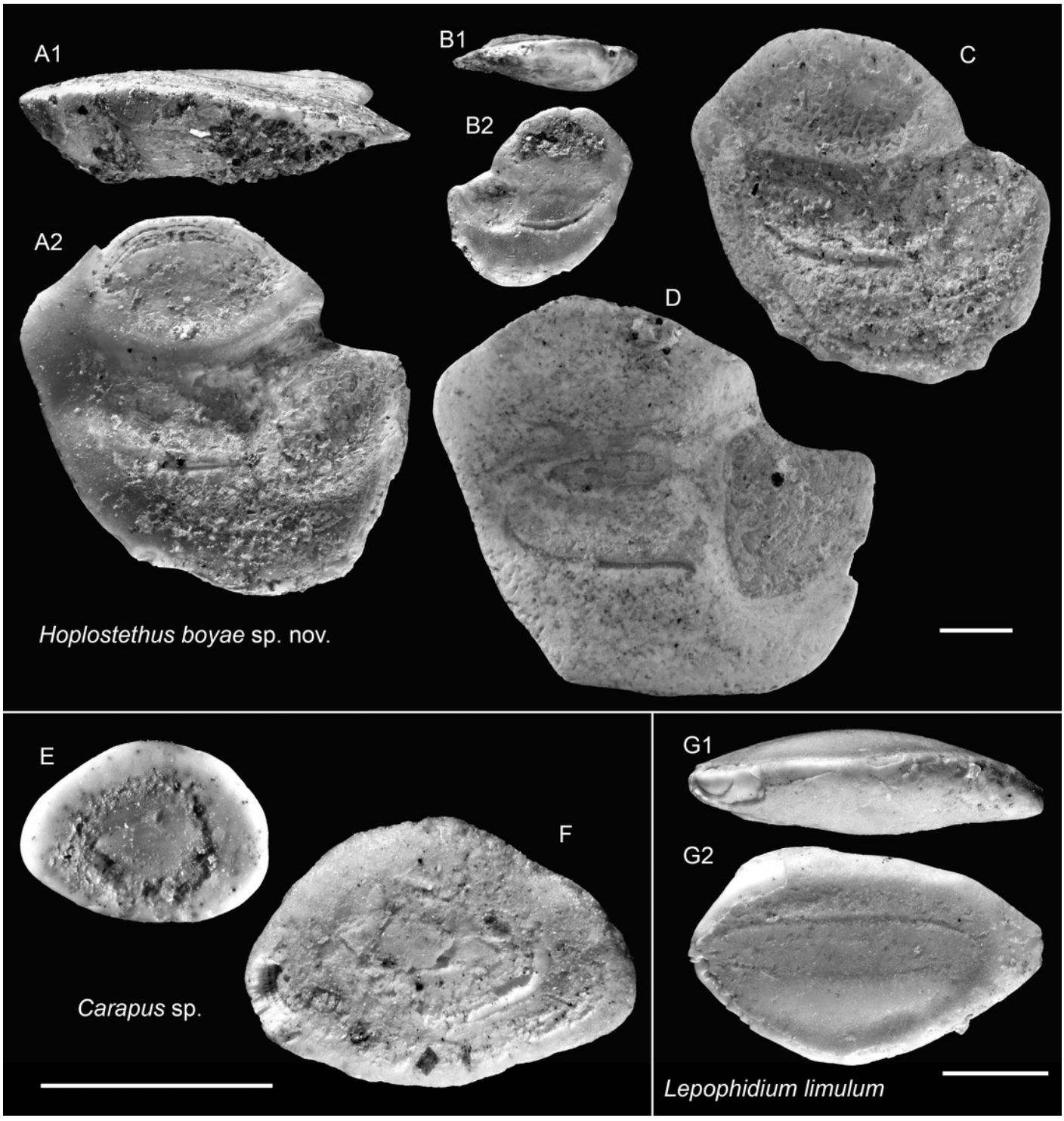
A1
B1
B2
C
A2
D
Hoplostethus boyae sp. nov.
E
F
Carapus sp.
G1
G2
Lepophidium limulum

Figure 11

Figure 11. Otoliths of Opistognathidae and Carangidae from the late Miocene Chagres Formation, Caribbean Panama.

(A) *Opistognathus* sp., ASIZF 0101013. (B) Carangidae indet., ASIZF 0101014. 1, ventral view; 2, inner view. Scale bar = 1 mm.

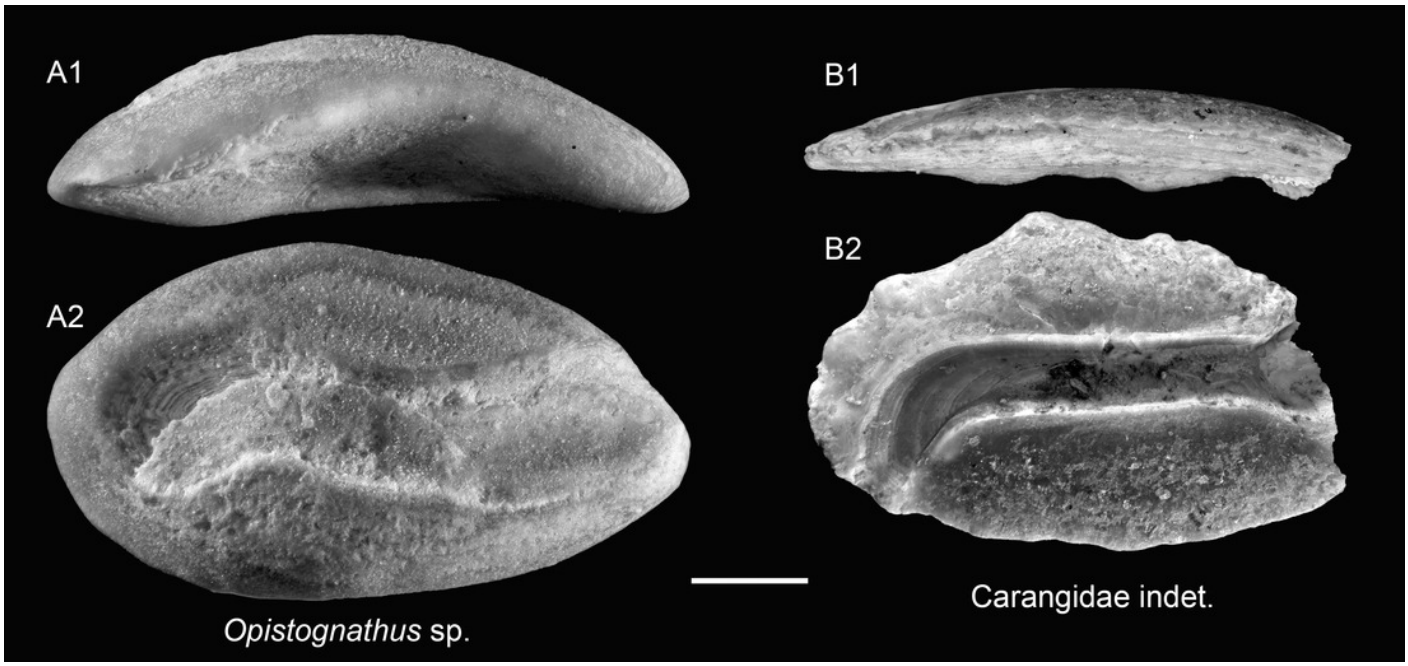

Figure 12

Figure 12. Otoliths of *Malakichthys* (Malakichthyidae) from the late Miocene Chagres Formation, Caribbean Panama.

(A–F) *Malakichthys schwarzhansi* sp. nov., (A) holotype, ASIZF 0101015, (B–F) paratypes, ASIZF 0101016–1020. Images are inner views unless otherwise indicated. 1, ventral view; 2, inner view. Scale bar = 1 mm.

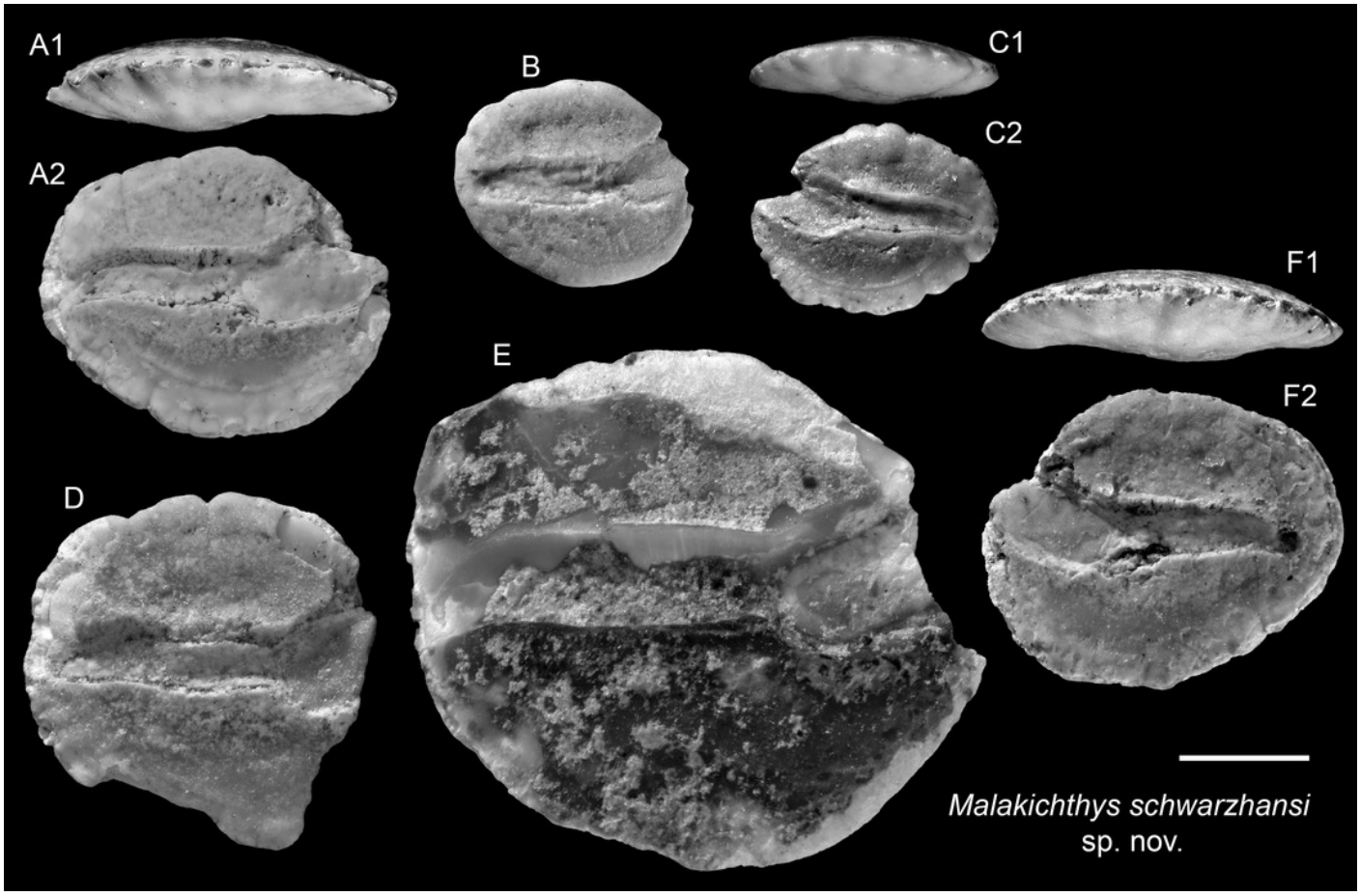

Figure 13

Figure 13. Extant *Malakichthys* (Malakichthyidae) otoliths.

(A and B) *Malakichthys wakiyae* Jordan & Hubbs, 1925, (A) 86.1 mm SL, CHLOL 10514, (B) 61.4 mm SL, CHLOL 10493. (C and D) *Malakichthys griseus* Döderlein, 1883, (C) 93.7 mm SL, CHLOL 14678, (D) 102.5 mm SL, CHLOL 34344. (E–G) *Malakichthys elegans* Matsubara & Yamaguti, 1943, (E) 131.9 mm SL, CHLOL 8241, (F) 62.9 mm SL, CHLOL 8800, (G) 77.8 mm SL, CHLOL 2605. (H and I) *Malakichthys formosus* Ng, Liu & Joung, 2023, (H) 72.1 mm SL, CHLOL 27488, (I) 64.9 mm SL, CHLOL 31419. (J–L) *Malakichthys barbatus* Yamanoue & Yoseda, 2001, (J) 161.0 mm SL, CHLOL 27489, (K) 83.51 mm SL, CHLOL 35072, (L) 223.5 mm SL, CHLOL 33087. Images are inner views unless otherwise indicated. 1, ventral view; 2, inner view. Scale bar = 1 mm.

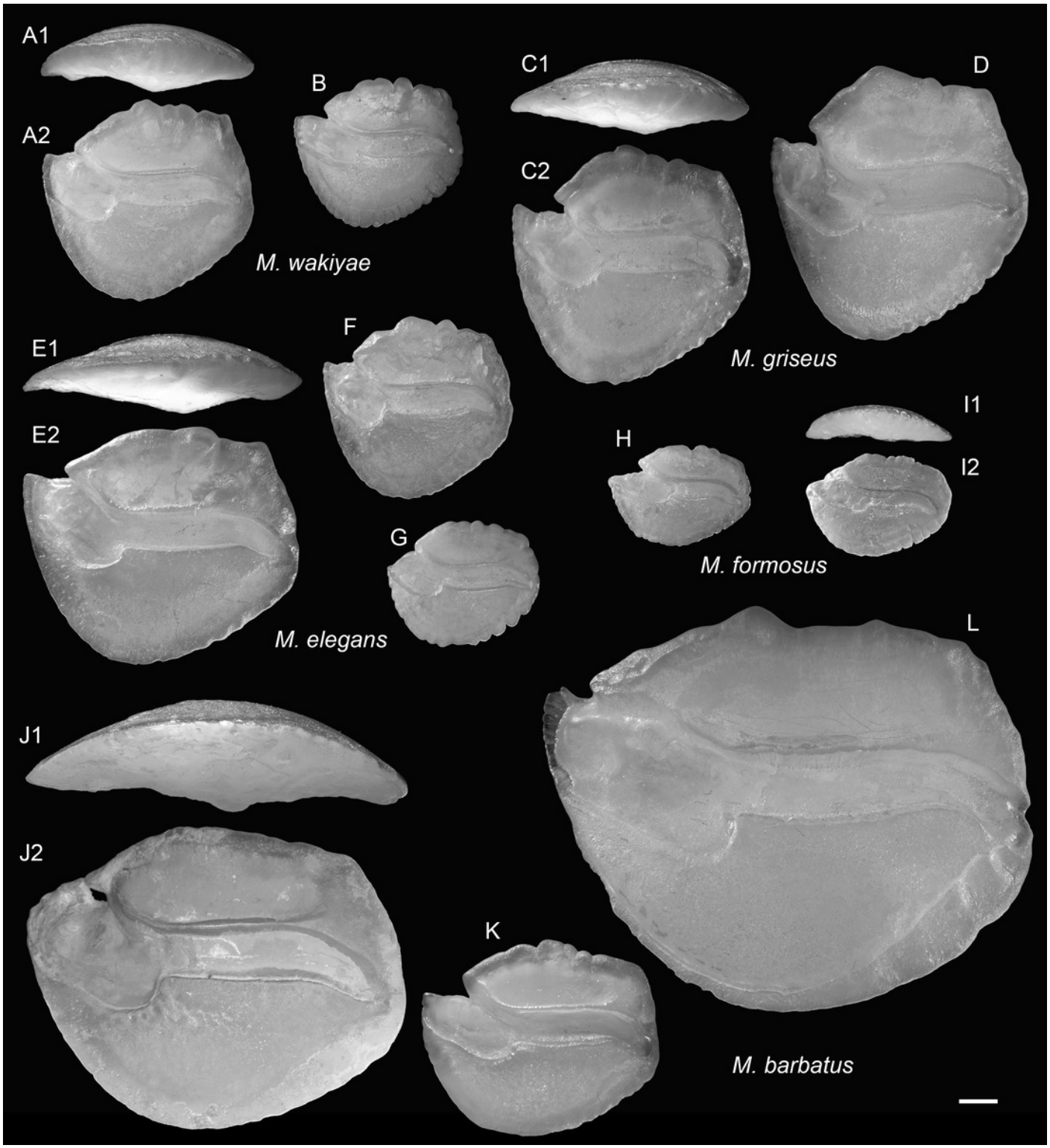
A1
A2
B
M. wakiyae
C1
C2
D
M. griseus
E1
E2
F
G
M. elegans
H
I1
I2
M. formosus
J1
J2
K
L
M. barbatus

Figure 14

Figure 14. Extant *Ambassis* (Ambassidae) otoliths.

(A) *Ambassis kopsii* Bleeker, 1858, 69.8 mm SL, CHLOL 28447. (B and C) *Ambassis miops* Günther, 1872, (B) 22.7 mm SL, CHLOL 31077, (C) 22.3 mm SL, CHLOL 31078. (D and E) *Ambassis urotaenia* Bleeker 1852, 1943, (D) 46.8 mm SL, CHLOL 27116, (E) 34.1 mm SL, CHLOL 27115. (F and G) *Ambassis interrupta* Bleeker, 1853, (F) 34.6 mm SL, CHLOL 27119, (G) 47.8 mm SL, CHLOL 27120. Images are inner views unless otherwise indicated. 1, ventral view; 2, inner view. Scale bar = 1 mm.

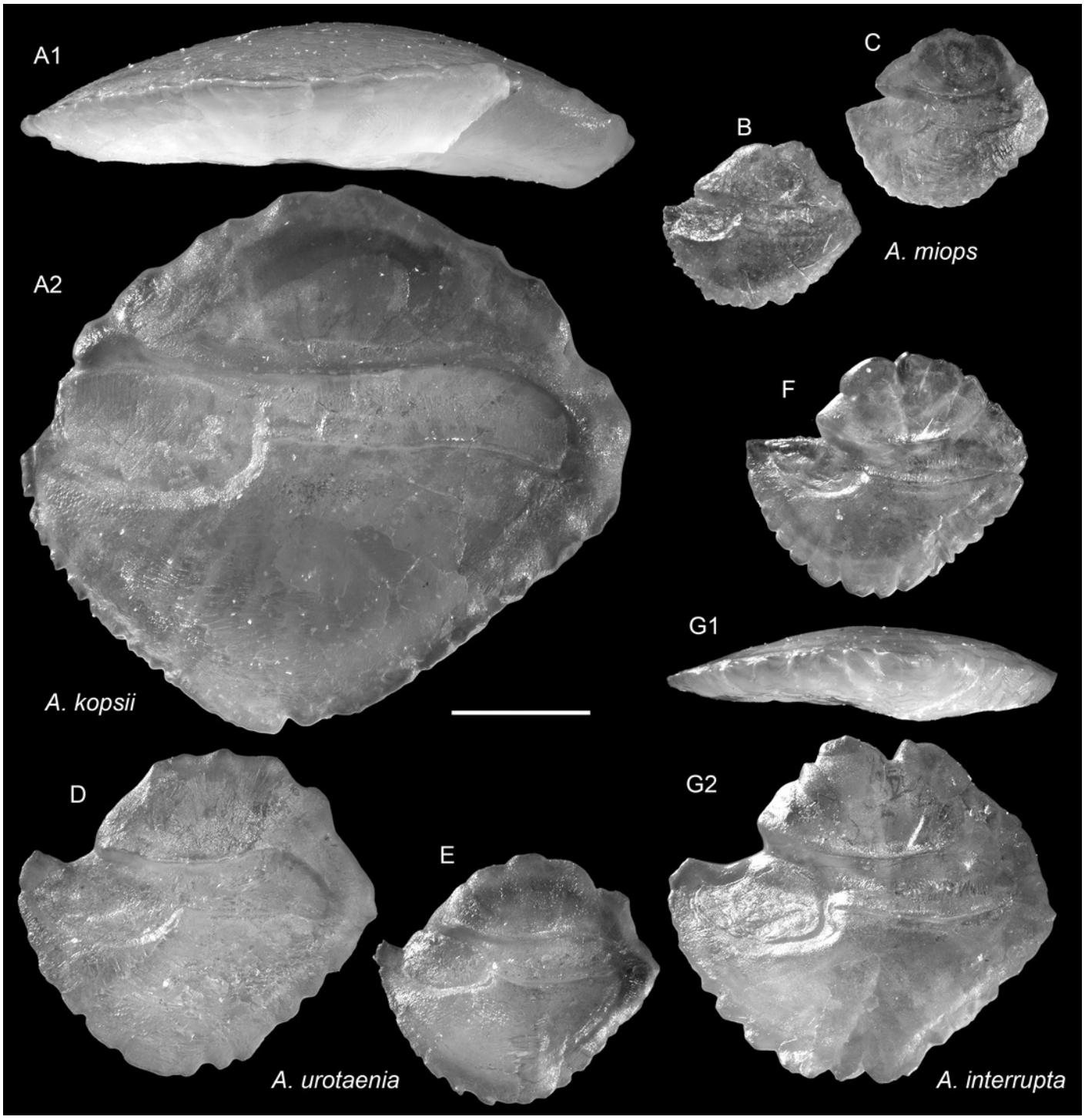
A1
C
B
A. miops
A2
F
G1
A. kopsii
D
E
G2
A. urotaenia
A. interrupta

Figure 15

Figure 15. Rank abundance of otolith families.

Note that y-axis is log-scaled, and the otolith counts are indicated in parentheses.

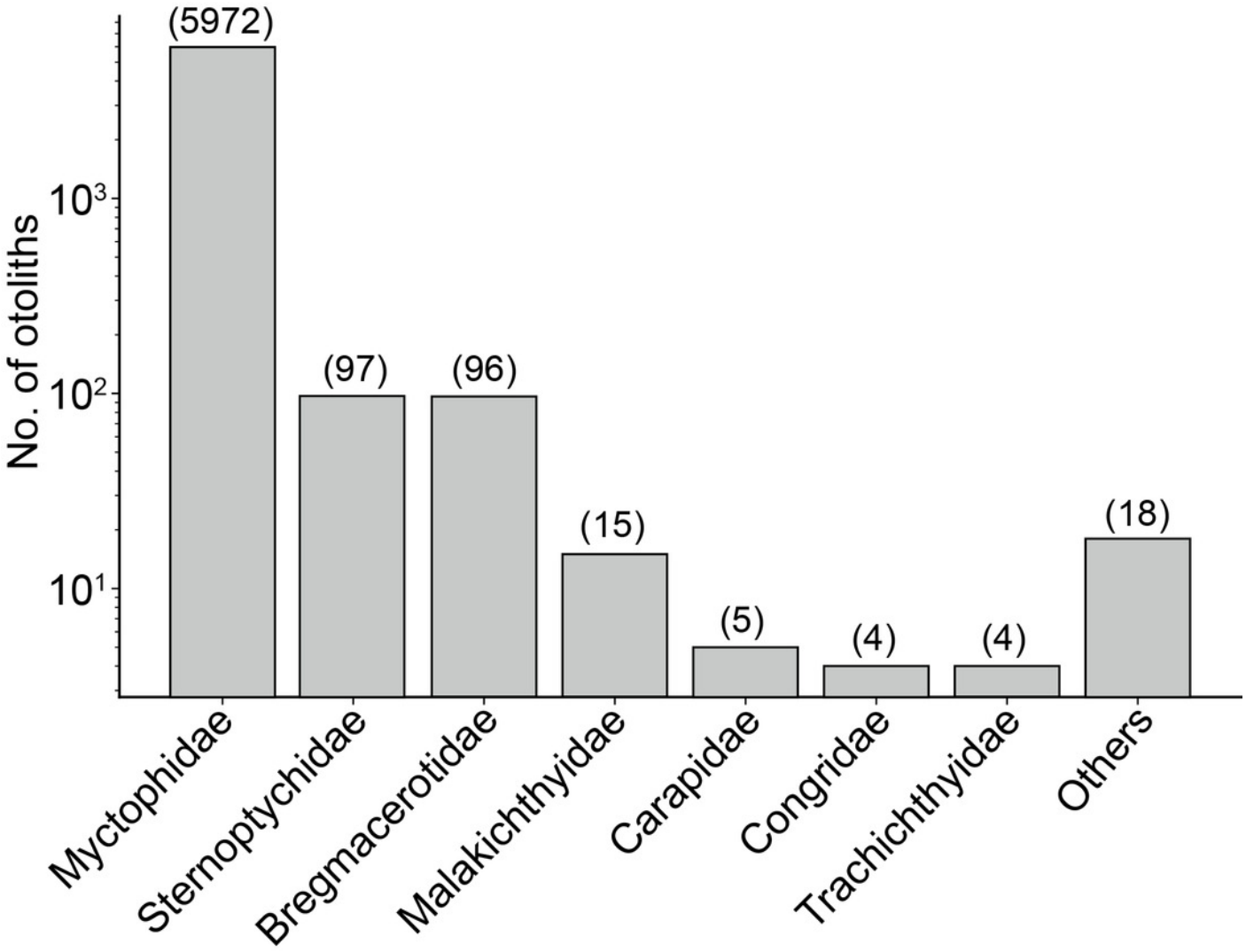

Figure 16

Figure 16. Rarefaction curves of otolith-based taxa (Hill numbers) represented by species richness (${}^{0}D$), Shannon diversity (${}^{1}D$), and Simpson (${}^{2}D$) diversity.

Shaded areas represent 95% confidence intervals based on 1000 bootstrap replicates.

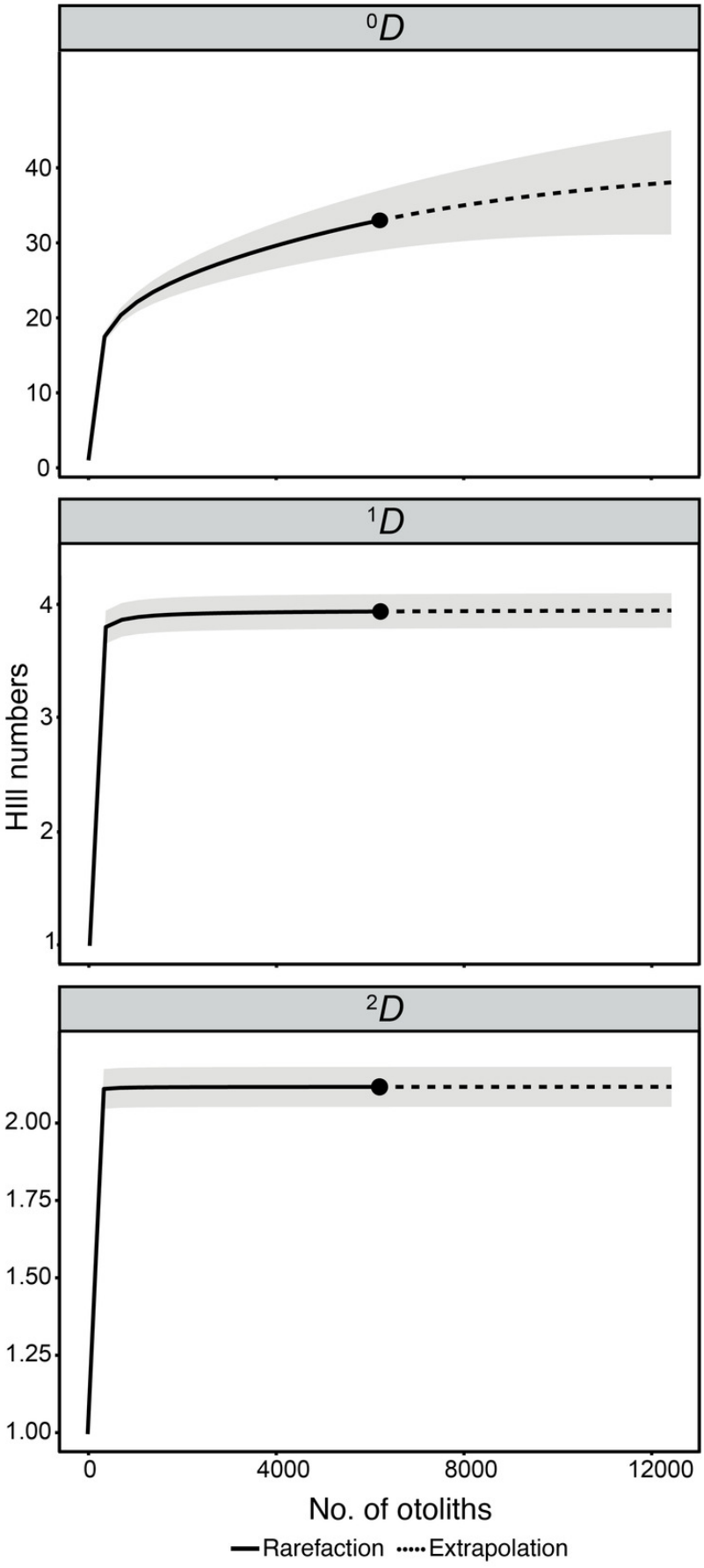
^0D
40
30
20
10
0
^1D
4
3
2
1
HIII numbers
^2D
2.00
1.75
1.50
1.25
1.00
0
4000
8000
12000
No. of otoliths
Rarefaction
Extrapolation

Table 1(on next page)

Table 1. List of otolith-based fish taxa from the late Miocene Chagres Formation, Caribbean Panama.

Family	Taxa	No. of otoliths
Congridae	*Chiloconger aflorens* sp. nov.	2
	Rhynchoconger sp.	1
	Congridae indet.	1
Argentinidae	*Argentina* sp.	1
Sternoptychidae	*Polyipnus* sp.	97
Myctophidae	*Benthosema pluridens* Schwarzhans & Aguliera, 2013	44
	Bolinichthys sp.	2
	Dasyscopelus degraciai (Schwarzhans & Aguliera, 2013)	256
	Dasyscopelus inopinatus sp. nov.	63
	Diaphus aequalis Schwarzhans & Aguliera, 2013	125
	Diaphus apalus Schwarzhans & Aguliera, 2013	152
	Diaphus barrigonensis Schwarzhans & Aguliera, 2013	39
	Diaphus dumerilii (Bleeker, 1856)	119
	Diaphus multiserratus Schwarzhans & Aguliera, 2013	26
	Diaphus pedemontanus (Robba, 1970)	78
	Diaphus rodriguezi Schwarzhans & Aguliera, 2013	780
	Diogenichthys sp.	1
	Lepidophanes inflectus Schwarzhans & Aguliera, 2013	9
	Lobianchia johnfitchi Schwarzhans & Aguliera, 2013	62
	Myctophum affine (Lütken, 1892)	13
	Myctophum arcanum Schwarzhans & Aguliera, 2013	24
	Myctophidae indet.	4179
Macrouridae	*Coelorinchus* sp.	2
	Macrouridae indet.	1
Bregmacerotidae	*Bregmaceros* sp.	96
Trachichthyidae	*Hoplostethus boyae* sp. nov.	4
Carapidae	*Carapus* sp.	5
Ophidiidae	*Lepophidium limulum* Schwarzhans & Aguliera, 2016	2
Opistognathidae	*Opistognathus* sp.	1
Carangidae	Carangidae indet.	2
Malakichthyidae	*Malakichthys schwarzhansi* sp. nov.	15
indet.	indet.	9
	total	6211

1